Glutamate Mediated Actions on Trace Memory: A Trimodal MRS-EEG-fMRI Imaging Study on Motor Sequence Learning

Shima Panahi Moghadam Namini

A Thesis

in

The Department

of

Electrical and Computer Engineering

Presented in Partial Fulfillment of the Requirements

for the Degree of

Master of Applied Science (Electrical Engineering) at

Concordia University

Montréal, Québec, Canada

October 2024

CONCORDIA UNIVERSITY

School of Graduate Studies

This is to certify that the thesis prepared

By: Shima Panahi Moghadam Namini

Entitled: Glutamate Mediated Actions on Trace Memory: A Trimodal MRS-EEG-fMRI Imaging Study on Motor Sequence Learning

and submitted in partial fulfillment of the requirements for the degree of

Master of Applied Science (Electrical Engineering)

complies with the regulations of this University and meets the accepted standards with respect to originality and quality.

Signed by the Final Examining Committee:

_____ Chair
Dr. Hassan Rivaz

_____ External Examiner
Dr. Christophe Grova

_____ Examiner
Dr. Hassan Rivaz

_____ Supervisor
Dr. Habib Benali

Approved by _____
Martin D. Pugh, Chair
Department of Electrical and Computer Engineering

_____ 2024

_____
Amir Asif, Dean
Faculty of Engineering and Computer Science

Abstract

Glutamate Mediated Actions on Trace Memory: A Trimodal MRS-EEG-fMRI Imaging Study on Motor Sequence Learning

Shima Panahi Moghadam Namini

Investigating motor memory formation and consolidation is a central endeavor of contemporary neuroscience as it helps to understand motor skill learning as well as how to treat its related deficits. Evidence from the current research shows that a short exposure to a motor skill learning task creates modifications in the neurophysiological and hemodynamical processes in the task-related brain areas which are considered as formation of new memory representations. These modifications occur mainly through excitatory-inhibitory synaptic changes which are partly associated with the modulation of glutamate (the main excitatory neurotransmitter in the central nervous system). Memory representations are susceptible to interference and can be diminished easily unless protected by a subsequent nap or overnight sleep in which the task-related neuronal activity will reappear and elicit plasticity. Eventually, behavioral enhancement can be expected after memory consolidation.

To further explain the motor skill learning in terms of the task-induced electrical, hemodynamic and metabolite activity of the human brain, we conducted a non-invasive study using multimodal brain imaging techniques under a motor sequence learning task whereby we could analyze the relationship between resting state spatiotemporal neuronal activity and the glutamate variations during one sleep-wake cycle. In this work, we demonstrated a conditional relationship between the dynamics of resting-state electrical activity and glutamate concentrations. This relationship was found in diurnal glutamate variations and Electroencephalography in the targeted Supplementary Motor Area in low gamma band (30-55Hz, p-value = 0.006) and overall band (0.5-55Hz, p-value = 0.014) as well as other motor network areas.

Acknowledgments

My journey through my M.Sc. studies has granted me the invaluable opportunity to learn from the expertise of many colleagues.

I extend my sincere acknowledgments to Pierre Berroir for his unwavering support and assistance in the implementation of this study. My deep appreciation goes to Makoto Uji for his guidance in setting up the EEG-fMRI system, training me on how to denoise EEG data acquired during fMRI using BrainVision Analyzer, and for always being available whenever challenges arose. I also wish to thank Ella Gabitov for sharing her expertise in the implementation of the MSL task, and a special thanks to Melodee Mograss for her training on the EEG international 10-20 system measurement. My sincere appreciation goes to my colleague Zhengchen Cai, for his collaboration in implementing the Linear Mixed Models in R software. I would also like to thank the students who supported our team during the 42-hour data collection sessions. My special thanks to Niusha Gomar for her assistance during the overnight data acquisition sessions, and to Edouard Delaire for his training on EEG digitization and setting up BrainVision Recorder.

My heartfelt gratitude goes to my supervisor, Habib Benali, for granting me the privilege of working with his team at the Biomedical Imaging and Healthy Aging Lab, for his constant guidance throughout the research process, for helping me navigate the path toward my M.Sc. degree, and for fostering a collaborative environment where I had the opportunity to work with many experts.

Last but not least, I would like to express my deepest gratitude to my beloved sister, Shirin, for her unwavering support and companionship throughout these years of international life; she is the glory of my heart, and of course to my beloved family, Fatemeh and Shadi, and my father's soul, Majid, who continue to be the lights of my life and will always remain in my heart.

I would like to dedicate this work to the Spiritual Mother, H.H. Shri Mataji Nirmala Devi, Who bestowed me my Sahaja Self-Realization.

Jai Shri Mataji Nirmala Devi

Contents

List of Figures

List of Tables

Chapter 1

Introduction

Motor control refers to the execution of a movement for the purpose of making a change in our environment. Motor skill learning is an outcome of motor control process and it refers to improvement of spatio-temporal accuracy of a movement through repeated practice. The movement itself can be a simple movement or a more complicated sequential movement in which order of performance matters. Movements can also be executed with a conscious effort and awareness of the goal or automatically in an unconscious mode. Depending on the behavior involved in a motor control process different brain areas can be allocated in performing a task. For example, dorso-lateral frontal cortex is involved when selecting goals and making a decision to change a target in the environment (strategic process) and it is known for coding the goal of movement. Posterior parietal lobe and premotor cortex can be involved when selecting a target for movement (perceptual-motor integration process). The supplementary motor area (SMA) and basal ganglia contribute to the planing of a sequence of movements (sequencing process). The spinal cord receives the signal of a new spatial and temporal pattern of movements via the primary motor cortex and a network of spinal interneurons translates it to a learned muscle activity (dynamic process) [1].

Memory formation is the process by which we can obtain progressive knowledge over time and express it as a learned behavior. Brain plasticity is a widely known mechanism of memory formation in which a change in neuronal properties will remain after exposure to a stimulus. The most well-known classification of memory formation is declarative memory versus non-declarative memory. Declarative memory is considered as the conscious memory for facts and past events

(i.e. learned ”what”) whereas non-declarative memory includes procedural memory (i.e. learned ”how”), for instance learning of skills or habits and it is considered as non-conscious. Declarative memory can be acquired with a few exposures to the information whereas non-declarative memory, i.e. procedural learning, for instance acquiring motor skills, requires longer periods of acquisition [2].

Like other instants of skill learning, motor skill learning also constitutes procedural memory which helps the retention of skills [3] and which makes possible the retention of learned connections between complex stimuli (sensory/perceptual input) and response chains (motor output) and adapting the responses based on the environment [2, 4].

One of the fundamental aspects of voluntary motor behavior is the ability to produce sequential movements. Motor sequence learning (MSL) is a type of motor skill learning in which a set of separate movements are learned through repeated practice until integrated into a unitary spatiotemporally connected sequence of movements [1]. MSL in humans is often assessed using two experimental paradigms: finger-to-thumb opposition sequence paradigm or sequential finger tapping paradigm. In the first paradigm, participants are asked to perform an apriori known (explicit task) 5-element sequence in a time window of 30 seconds whereas in the second paradigm, participants are asked to learn a new sequence of finger tapping explicitly or implicitly (i.e. to repeat an unknown sequence for as long as they see a stimuli displayed on a computer screen) [5].

Memory formation is a developing process by which knowledge is acquired and modified during time which eventually results in retention of a memory. The time course of changes in brain plasticity can be within seconds during performing a task, minutes after performing the task or more delayed, in the subsequent hours or days after the task. In procedural memory, following the first exposure to a task, a memory representation of the information or a memory trace is formed in the brain which later will evolve in different stages. The process of transformation of a fragile memory representation into a more robust and stable memory which resists to interference (physical, pharmacological, experimental interventions, etc.) is considered as memory consolidation [2, 6].

The most distinguished memory formation phases are the initial acquisition phase (fast stage) following a consolidation phase (slow stage) [2, 3]. In procedural memory, since the behavioral performance improves within a session of repeated practice and task proficiency is acquired during

the first exposure to the paradigm, the initial acquisition involves learning [2].

Results of previous studies on motor skill learning have shown after the initial acquisition, once a time window has passed in an awake resting state, a time-dependent memory stabilization process takes place in which no additional learning improvements occurs, but the performance level maintains relatively the same to the post-training performance level [2, 7, 8]. This phenomenon is considered as the stabilization part of procedural memory consolidation which is time-dependent and occurs in the waking episodes after performing the task [2].

The evidence from other studies on sequential finger-tapping task [3, 9] suggests after performing the task, resting -including sleep episodes- enhances the performance level rather than just maintaining it, which is considered as the enhancement part of procedural memory consolidation which is sleep-dependent [2]. Thus, in procedural learning memory consolidation is not only a time-dependent process but also it depends on wake and sleep episodes.

The evolution of MSL is also characterized at least by these two distinct stages: the fast stage, and the slow stage [3, 5, 10]. The fast learning stage occurs during the first exposure to a new motor task in which an improvement in performance is acquired within one session of practice. The slow learning stage comes later after several sessions of practice in which a small and steady improvement in performance is acquired over a longer period of practice i.e. days, weeks, months or years [11].

In addition to fast and slow phases of procedural learning, the results of numerous studies now indicate that a spontaneous improvement in performance can be observed without any additional practice after the first sleep post training (i.e., offline). This phenomenon is also attributed to the enhancement process of consolidation and is susceptible to interference by a subsequent experience [2]. A study on sequential motor learning showed that the expression of delayed offline performance gain after 24 hours can be prevented by an interference experienced 2 hours post training. However, taking a 90-minute nap right after the training protected the expression of delayed offline gain from diminishing; after taking the nap, in the case of no interference, the expression of delayed gain occurred within 8 hours post training and in the case of presence of an interference after the nap, still robust delayed gains were expressed overnight. These results indicate the sensitivity and dependence of formation and consolidation of a procedural memory representation to the sleep

process [5].

The MSL integrates at the cortical, subcortical and spinal cord levels during each of the fast and slow learning phases. Based on the nature of the task (explicit or implicit), the brain structures that are engaged during the fast learning phase are the striatum, the cerebellum, the hippocampus, the spinal cord, motor cortical regions (e.g. premotor cortex, SMA, pre-SMA, anterior cingulate), prefrontal and parietal cortical areas. However, when MSL is practiced repeatedly over the course of time (sessions, days, months, etc.) and enters the slow learning phase, a time and sleep dependent consolidation process starts until the MSL is learned completely; Hence, the MSL will involve a network of brain structures including the cortico-striatal circuit (i.e. striatum, motor cortical regions and parietal cortices) that seems to be reactivated while retrieval and further practice [5].

MSL related brain networks are thought to be reactivated during the subsequent sleep evoking the sleep-dependent plasticity and enhancing the forthcoming learning behaviour [12].

One of the events that are thought to reflect a neuronal mechanism associated with memory consolidation during sleep is sleep spindles which propagate in thalamo-cortical networks and characterize non-rapid eye movement (NREM) [13]. For instance, results of a study [14] showed that sleep dependent motor learning have a positive correlation with stage 2 NREM sleep when the spindle density reaches its peak. Another study [15] also demonstrated an increase in the duration of stage 2 sleep, the density and the average duration of sleep spindles during the night after performing the motor task compared with the spindles found during the night before the training. Findings of a recent study [16] in motor skill learning confirmed the critical role of stage 2 NREM sleep spindles in memory consolidation providing evidence that sleep spindles locally reactivate and bind (functionally) specific task-relevant regions and synchronize the specialized cortical and subcortical networks including the motor-related cortical regions, the hippocampus, putamen and thalamus.

One question that arises here is that how the brain initiates the new memory formation and how these memories are selected for consolidation which takes us to take a deeper look at what is happening at the neuronal level.

One of the processes that modulate the synaptic sensitivity is synaptic potentiation by which either an enhancement in synaptic sensitivity over time occurs that is called long-term potentiation (LTP) or a reduction of synaptic sensitivity or synaptic depotentiation occurs that is called long-term

depression (LTD).

Synaptic strength takes place during LTP, when a presynaptic neurotransmitter is released at the same time as the excitation of a postsynaptic action potential. In the absence of a postsynaptic action potential or its coincidence with the presynaptic modulation, LTD occurs in the synapse. LTD has an important role in synaptic plasticity as continuous potetiation will result in an inefficient network [2]. In different brain structures, LTP and LTD use different mechanisms such as variation in neurotransmitter release, modulation of neurotransmitter receptors, regulation of gene expression and protein synthesis, etc. and cause the prolonged changes in synaptic strength which contribute to learned behaviour and memory processes [17].

During wakefulness, the interaction with environment and acquisition of the information increase the total synaptic strength in a large fraction of cortical circuits through the induction of LTP-related molecules that are connected with wakefulness whether or not there is an involvement in learning paradigms. In adults, any plastic changes that occurs during wakefulness would results in LTP more than LTD which contributes to a net potentiation of synaptic strength during wakefulness. The sensory, motor and cognitive activity during wakefulness have high peak firing rates also causing the increase of total synaptic strength. Some of the neuromodulatory systems only fire during wakefulness and are almost absent or low during sleep [18]. Increased synaptic strength results in higher energy consumption, demand for cellular supplies for synapses, cellular stress, and related changes in support cells (e.g. glia cells); it reduces the selectivity of neuronal responses and at the system level, it saturates learning by the time of sleep [19].

In order to restore the cellular function and the selective responses, neurons must renormalize the total synaptic strength through the LTD. The synaptic homeostasis hypothesis (SHY) by Tononi and Cirelli, 2006 [18], proposes that the regulation of synaptic strength happens during sleep through the synaptic depression. During sleep, the spontaneous activity of the brain downscales the synaptic strength to a baseline level, reduces the plasticity load on the neurons and supporting cells leading to restoration of selectivity and desaturation of plasticity which eventually results in restoration of energy and supplies, makes efficient use of gray matter space and helps consolidation and memory integration by enhancing the signal to noise ratios. Thus, sleep helps the homeostatic regulation of the total synaptic weight on the neurons [19].

Neural excitation and inhibition in the brain is mediated through glutamate (Glu) and Gamma-aminobutyric acid (GABA) as the main excitatory and inhibitory neurotransmitters respectively. Their physiological balance in the brain is homeostatically regulated [20].

Extra-synaptic glutamate (eGlu) originates from the sources in the central nervous system; it emanates from the release from the astrocytes and microglia cells. EGlu involves the astroglia cells to regulate the neuronal excitability and synaptic strength which contributes to neurosecretion, neuromodulation, memory formation, learning and sleep homeostasis [21, 22].

Apart from the synaptic homeostatic regulation, it has been shown that in the existence of external inputs such as motor learning, the induction of dynamic responses of Glu and GABA are vital to plasticity. This is because the modulation of glutamatergic and GABAergic processes after learning induce the LTP that is associated with synaptic strengthening and memory formation [23].

Glutamate and GABA as the main neurotransmitters involve in excitatory and inhibitory processes and metabolic activity of the brain can be measured in localized and task-related brain areas using functional proton Magnetic Resonance Spectroscopy (^{1}H fMRS) [20, 24]. Using MRS, different studies have provided insight to the excitatory and inhibitory role of Glu and GABA in motor learning paradigm as well as other sensory or perceptual paradigms.

In 2009, a study on rats cerebral cortex demonstrated the effect of sleep wake cycle on the neuronal firing and the variations in the cerebral metabolism. They provided evidence that during wake episodes and REM sleep glutamate concentration increases progressively and decreases during NREM sleep [25].

In 2007, a study in the visual paradigm on 12 healthy subjects aged 19 to 26 measured the concentrations of seventeen metabolites during two visual tasks at 7T and observed a significant increase in lactate and glutamate and decrease in aspartate implying an increase in oxidative metabolism during a task suggesting the effect of physiological stimulation on the amino-acid homeostasis [26].

In 2014, a study in motor paradigm on 11 healthy subjects of age 18 to 26 demonstrated a significant increase in metabolite activity of the human brain during execution of a motor task (finger-to-thumb tapping task) using 7T fMRS; From the glutamate and lactate rise, they inferred this increase might be associated with the increase in the neuronal activity [27].

In 2018, another study on 16 healthy subjects of age 18 to 30 investigated this approach in the

working memory cognitive task performance which is known to excite dorsolateral prefrontal cortex (dlPFC); under 3T fMRS, they found out an increase in dlPFC glutamate concentrations modulated by the working memory cognitive demands [24].

In 2015, a study on 40 healthy subject of mean age 23.8 tested the changes in network level functional connectivity and the local inhibition (under 3T) in the primary motor cortex (M1) in a motor skill learning paradigm (ball juggling) under different intensities and before and after 6 weeks of training. Result of this study suggested that the training intensity had an impact on the formation of distinct patterns of learning related change in resting state brain networks which was negatively correlated with GABA concentrations [28].

In 2018, a study on 34 healthy participants of mean age 24 was investigated under 7T MRS for the variations of GABA in primary motor cortex during motor learning. MRS was acquired during a concurrent task; for the learning group, a repeating serial reaction time task (SRTT) consisting of 16 key press in each block, for the movement controlling group, a SRTT without repeat and for the rest group observation of a video were considered. They observed a significant reduction over time in M1 GABA as well as the reaction time (RT) in the learning group. Also they found out that the lower levels of GABA is correlated with a greater reduction in RT [29].

In 2018, a study on 55 healthy volunteers of mean age 27.3, merged with the neuro-imaging (fMRI-MRS) data of an earlier study with 25 healthy subject of mean age 27.4, was conducted under 3T MRS and fMRI under rest and increasing visual input as well as task stimuli and investigated glutamate and GABA levels in the visual cortex. They found that when opening the eyes in darkness, GABA levels will decrease whereas the glx (glutamate and glutamine) will stay stable; when adding the visual stimuli, the glx will increase. Therefore, they suggested that differences in brain states can be detected in contrasting Glx and GABA dynamics [30].

In 2023, a study on 9 healthy subjects of age 18 to 40 was conducted under 3T MRS with a motor sequence learning task using the right hand. Participants were scanned twice a day, at a resting condition before the task and while performing the task; They were scanned on two different days, 1 week apart, for the baseline (movement condition) and learning condition. In this study, no significant change in GABA+/tCr (total Creatine), Glx/tCr, or Glu/tCr were reported, however, they showed that there was a positive relationship between glu levels and motor (sequence) learning at

rest as well as the start of the task [31].

In 2024, a study on 57 healthy individuals of mean age 27.5 was conducted under 7T MRI for a motor sequence learning task using the left hand. Participants were divided into two groups of control (n=21) and learning (n=36) and were scanned for MRS and fMRI in two consecutive days. The control or MSL task was performed during the fMRI and the MRS was performed before and after the task. The second day also included resting state fMRI and MRS before performing the task under the last fMRI acquisition for the learning group and no task for the control group. The result of their study showed short-term (within 30 minutes after the task) glutamate and GABA signaling in M1 were associated with long-term (overnight) learning induced brain modifications (in structure, function and behaviour) which indicates the role of glutamate and GABA in motor memory formation and consolidation [20].

There are numerous studies done on memory formation and consolidation in motor system in human brain using different imaging modalities that connects glutamate and GABA variations (MRS) in the motor system with the behavioral motor learning or with the blood-oxygen-level-dependent (BOLD) signal (fMRI) in short-term and long-term memory acquisitions; However, there is little evidence explaining the neurons' electrical activity (EEG) based on the metabolite variations (MRS) in motor memory formation and consolidation at least during the first day of memory acquisition including the wake and sleep episodes.

Considering glutamate as the main excitatory neurotransmitter that is increased within the neuronal population after performing a motor task, we designed and conducted a study to find the relationship between the electrical activity of the brain (EEG) and the glutamate variations (MRS). Focusing on the resting state brain activity during one sleep wake cycle, we tested the participants at multiple instants using EEG-fMRI and MRS either at rest or under the two task conditions of motor sequence learning or no learning to find the relationship between the electro-physiological and hemodynamic neural activity in its circadian variation and under the modifications induced by the task.

In this particular thesis work and for the first time, I will present part of the results associated with the correlation of EEG and MRS data as well as task induced changes in EEG.

Chapter 2

Methodology

In this study, we are investigating the effects of motor sequence learning (MSL) task on the glutamate concentration and brain activity right after the task in the specific ROIs using non-invasive multimodal imaging techniques including Electroencephalography (EEG), Magnetic Resonance Spectroscopy (MRS) and functional Magnetic Resonance Imaging (fMRI) that will allow to monitor bioelectrical, biochemical and hemodynamic activity of the brain.

The glutamate concentration has a homeostatic circadian-like rhythmicity; it has been shown that during the day, cortical glutamate levels increase progressively in the rat and human cortex [25, 32]

Here, the hypothesis is that the MSL task will increase the glutamate concentration levels in the Supplementary Motor Area (SMA) more than the global increase that occurs in the circadian-like rhythmicity of glutamate levels during the day. In this work, I particularly investigated these task-related variations in electrical activity of the brain and its association with the variations in glutamate concentration.

During the night, glutamate level is expected to increase during REM sleep and decrease during NREM sleep [25]. Memory consolidation occurs with the sleep spindles of NREM sleep [33]. The increase in the number of sleep spindles in SMA and PCC during sleep may play a role in memory consolidation. The data analysis of this part is not included in the current thesis.

2.1 Study Design

We tested the hypothesis by quantifying the glutamate levels and the neuronal activity in one sleep wake cycle. Below, I explain about the learning conditions, number of acquisitions, the MSL task, the ROIs and the technical aspects of running the protocol.

2.1.1 Control Day vs MSL Day

Two days and two conditions were considered for the means of comparison:

(1) First day visit consisting of resting state sessions and simple motor task sessions without high cognitive demand for learning before going to the scanner. For the sake of simplicity, we call this visit the Control day.

(2) Second day visit consisting of resting state sessions and complicated MSL task sessions with a higher cognitive demand for learning before going to the scanner. This visit also included an overnight stay in the lab. For the sake of simplicity, we call this visit the MSL day.

The variations of glutamate and the neuronal activity were quantified under the two conditions of no learning (either resting or doing the control task for monitoring movement effects) and sequence learning for each participant in the two visits which were two or three weeks apart and the order of the two visits was counterbalanced across participants. For each participant, the brain variations in the MSL day is compared to the Control day as this is a within-subject analysis. The Control and MSL tasks were done before going to the scanner and all the data collection were done in the scanner while participants were resting.

2.1.2 Experimental Design and Number of Acquisitions in Practice

This study consisted of two visits of a total 42hrs per participant: Control day (16hrs) and MSL day (26hrs) shown in Figure 2.1.

Data collection during MSL day consisted of six data acquisition sessions including EEG-fMRI and MRS at different time points at 9:30, 11:30, 13:30, 17:30, 21:30, 9:30 (day after). Participants

performed the MSL task three times at 10:30 and 16:30 (before going to the scanner), and at 10:30 the day after (after going to the scanner).

To characterize the circadian rhythm, melatonin was measured at 8:00, 13:00, 17:00, 18:00, 19:00, 20:00, 21:00, 22:00, 8:00 (day after) and cortisol was measured at 9:00, 11:00, 13:00, 17:00, 19:00, 8:00 (day after) during waking hours and 40 minutes post-awakening.

For monitoring sleep, polysomnography (PSG) was also measured unimodal at 23:00 to 7:00.

Data collection during the Control visit was similar to the MSL visit except that participants were asked to leave the lab after the fifth scan. The task in the Control day was without any cognitive demand for learning and it was performed twice at 10:30 and 16:30 (before going to the scanner) to control for the finger movements.

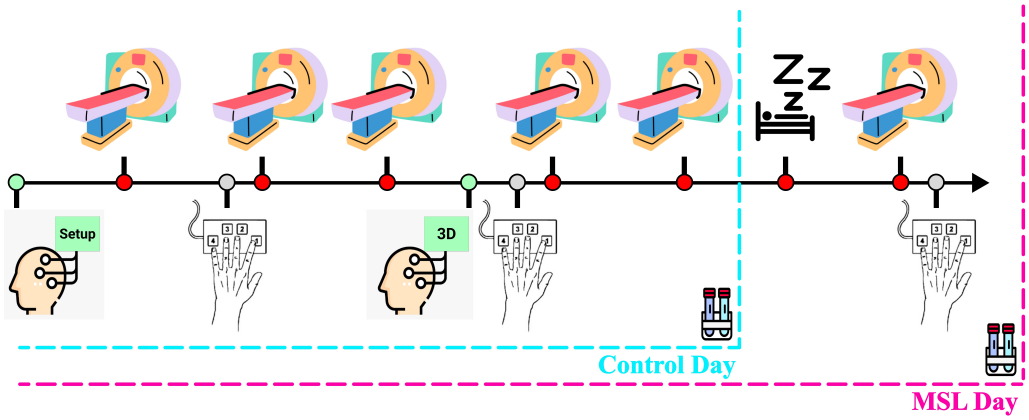

Figure 2.1: Schematic of the protocol for the MSL and Control days. Each MRI icon indicates resting state (rs) MR scans (T1, 10 min rs-EEG-fMRI, 10 min rs-MRS in SMA and 10 min rs-MRS in PCC). Each left hand icon represents performing the Control/MSL task before the subsequent MR scan during the first day. MSL day includes sleep monitoring using overnight PSG, a last MR scan and performing the MSL task the day after for testing memory consolidation. The icons "setup" indicates EEG free electrodes setup using collodion upon arrival in early morning. The icon "3D" means EEG free electrodes digitization. The vials icon indicates sampling melatonine and cortisol at multiple instances during each day.

2.1.3 The Motor Sequence Learning (MSL) Task

We took advantage of an implicit MSL task using a finger-tapping paradigm shown in Figure 2.2. Each participant was asked to sit comfortably in front of a computer screen with a response box placed in front of them on the desk under their left (non-dominant) hand. The response box

consisted of four pressing keys with the keypress number one being assigned to the index finger, number two the middle finger, number three the ring finger and number four the little finger.

During the MSL day, the task consisted of repeating an unknown eight element finger-tapping sequence for as long as a green sign was shown on the screen and each two consecutive blocks were separated with 30 seconds of rest. The performance duration for each key press was recorded using the response box. The MSL task was done three times during the MSL day:

(1) Before the second scan (First time exposure to the task consisting of ten block of repetition)

(2) 6hrs later before the forth scan (recall the sequence consisted of eight blocks of repetition)

(3) 24hrs later after the last scan (test for consolidation consisted of eight blocks of repetition)

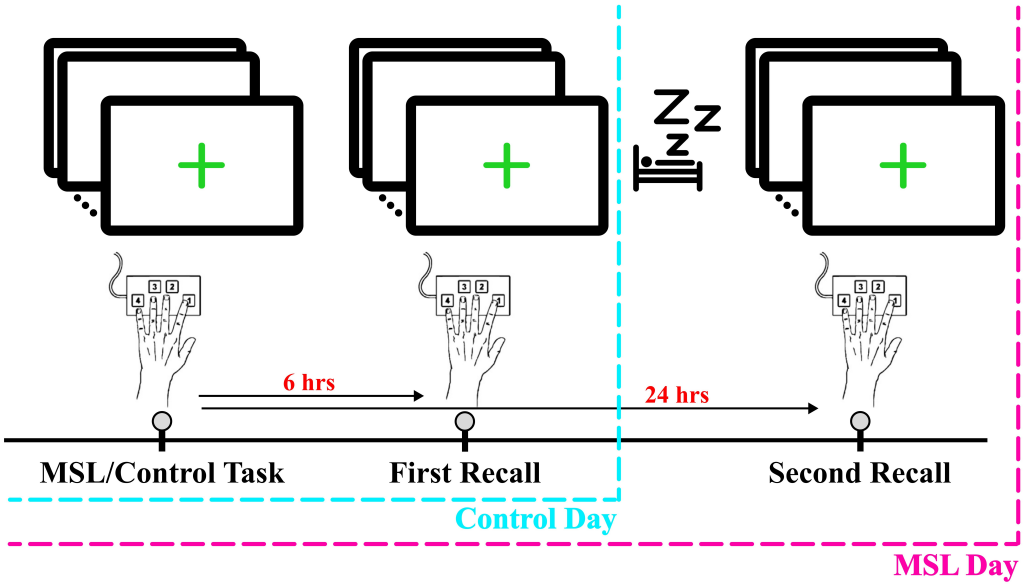

Figure 2.2: Schematic of the MSL or Control task design. Participants were asked to perform the task using their left (non-dominant) hand and a response box on which number one was assigned to the key under the index finger. On MSL day, the MSL task was to repeat an implicit sequence for as long as the green sign was shown on the screen. Between the repetition blocks there was 30 seconds rest periods and the sequence was repetitive after the first exposure (became explicitly known). The first and second time performing the task was 6 hours apart to avoid interference with learning and on MSL day, the task was performed again after 24 hours (post sleep) to test the behavioral consolidation. On Control day, the task was just finger-tapping to control for movement impacts in contrast with resting and MSL conditions.

During the Control day, the task consisted of a finger-taping task without any particular sequence

to learn just to control for the fingers motor activity and to prevent any neuronal firing and learning effects in the ROI (SMA) associated with the sequence learning. The Control task was done twice during the Control day:

(1) Before the second scan

(2) 6hrs later before the forth scan

2.1.4 The Brain Areas of Interest

To analyze the glutamate and neuronal activity variations, two brain regions were targeted:

(1) The Supplementary Motor Area (SMA), which is known to be involved in MSL [34] shown in Figure 2.3,

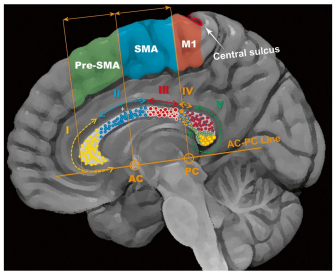

Figure 2.3: Pre SMA, SMA and Primary Motor cortex (M1) [35]

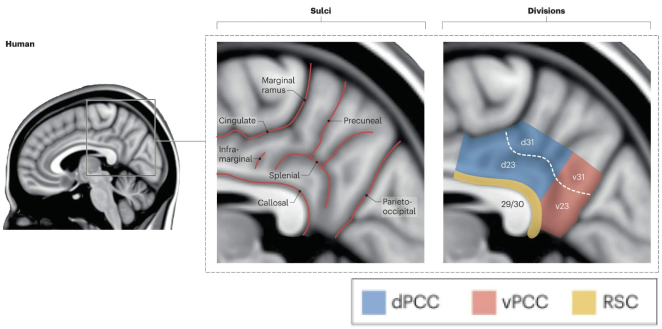

Figure 2.4: Anatomy of PCC including dorsal PCC (blue) and ventral PCC (red) adapted from [36]

(2) The Posterior Cingulate Cortex (PCC) as a control region, which is known to be involved in sleep homeostasis [37, 38] but not in motor learning [20] shown in Figure 2.4.

2.1.5 Acquisition Modalities

Magnetic Resonance Spectroscopy (MRS)

MRS is a non invasive MR imaging technique which allows for studying various metabolites and physiological information in the human body using different nuclei, for instance ^{1}H, ^{31}P, ^{19}F, ^{13}C, ^{23}Na. The sensitivity, availability and abundance of the ^{1}H in most metabolites makes it the most common isotope that is used in MR spectroscopy. Another reason that supports the use of ^{1}H MRS in comparison to other isotopes is that it can be performed using the standard MRI scanners with conventional Radio-Frequency (RF) coils developed for the acquisition of clinical MR images and without the need for any hardware modifications. Unlike the MR images that are acquired from the signal of ^{1}H in water and fat, in MRS the ^{1}H signal from smaller metabolites are of interest; thus, having a sufficient field strength of above 1.5 T is necessary and will provide a signal with acceptable SNR [39, 40].

For the MRS data collection, first an anatomical MRI is performed and using the MR images a single volume of interest from the tissue will be selected to acquire the metabolite spectrum.

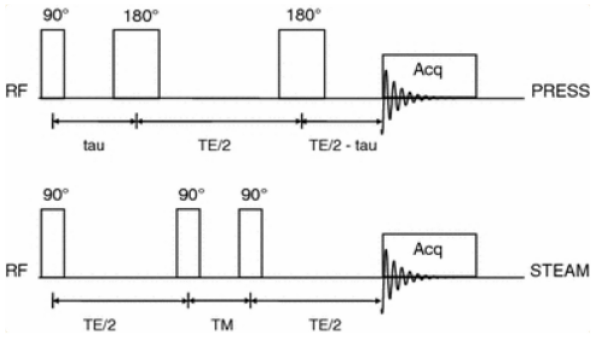

Figure 2.5: PRESS and STEAM pulse sequences [39]

There are two techniques for ^{1}H MRS data collection in the brain shown in Figure 2.5:

(1) Point REsolved SpectroScopy (PRESS) in which an echo is obtained by a 90° excitation pulse followed by two 180° refocusing pulses

(2) STimulated Echo Acquisition Mode (STEAM) in which an echo is obtained by three 90° pulses

In both methods each of the three pulses will be combined with an X, Y, Z direction gradient which allows to select a slice and the overlapping slices will allow to select a rectangular volume or a single voxel.

The echo time (TE) can be changed by modifying the delay times between the pulses. A shorter TE will allow to obtain signals with minimum loss whereas a longer TE will allow to obtain signals with a limited number of sharp resonances. An example of metabolites in a single-voxel MRS obtained at different short and long TEs is shown in Figure 2.6.

When collecting the spectra, a technique called CHEmical Shift-Selective (CHESS) water suppression is employed to suppress the water signal from the metabolite. And the spectra is acquired with and without water suppression for line-shape correction [39].

In the current study, we used PRESS (with and without CHESS) technique to collect the glutamate concentrations in SMA and PCC areas at various times during wakefulness while participants were resting in the scanner.

Electroencephalography (EEG)

To measure the bioelectical activity of the brain, before each MRS scan, a simultaneous EEG-fMRI was acquired while participants were resting in the scanner.

During the second visit, a unimodal EEG was also used to record participants' sleep or Polysomnography (PSG) for future investigations to detect MSL sequence-specific reactivations, as well as sleep stages and to determine whether the motor plasticity relates to sleep spindles activity. For monitoring PSG, two electrodes were installed around the eyes to record the Electrooculogram (EOG).

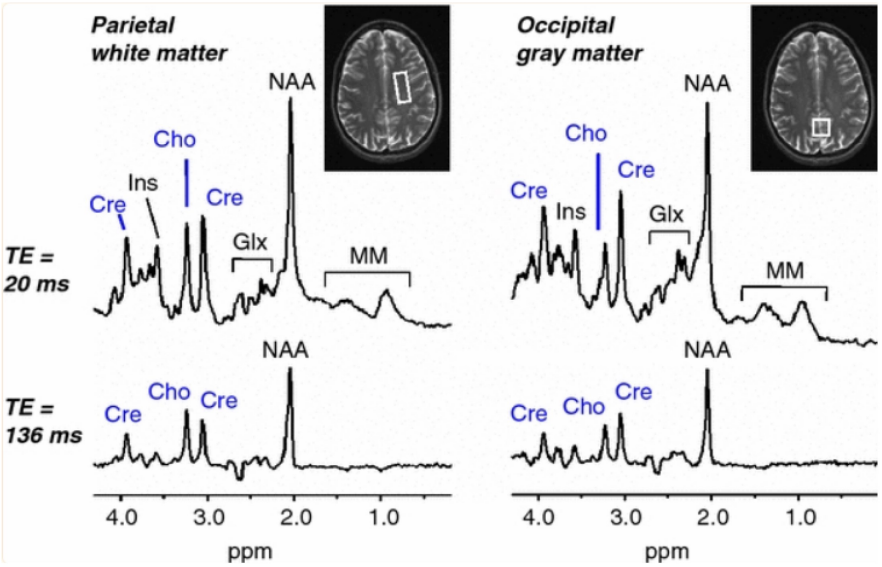

Figure 2.6: Example of a healthy subject's single-voxel MRS obtained at 3T from white matter (left) and gray matter (right). Spectra were obtained with PRESS volume selection (TE/TR = 20/5,000 ms for upper row and TE/TR = 136/2,000 ms for lower row). The prominent metabolites are labeled: creatine (Cre), myo-inositol (Ins), choline (Cho), glutamine and glutamate (Glx), N-acetyl aspartate (NAA), macromolecules (MM). In blue the relative signal intensities of Cho and Cre are shown. These metabolites are measured in parts per million (ppm) [39]

Functional Magnetic Resonance Imaging (fMRI)

To quantify the degree of involvement of the SMA and PCC in the intrinsic functional networks of the brain, fMRI was used bimodal with EEG before each MRS scan while participants were resting in the scanner.

2.2 Technical Design for Imaging and Data Collection

2.2.1 Magnetic Resonance Imaging (T1, fMRI and MRS)

Brain MRI data was acquired using a 3.0T GE MRI Scanner and a 32-channel head coil at Perform Center.

Anatomical MRI (T1)

A high-resolution structural T1-weighted MRI image was acquired using an MPRAGE pulse sequence (TR = 13ms; TE = 4.92ms; FA = 25°; FoV = 256x256 mm^2; matrix size = 256x256; voxel size = 1x1x1 mm^3, 176 slices). A field map, acquired using a double echo gradient. Echo sequence was also used to correct for geometric distortions due to magnetic field non-homogeneities.

Functional MRI (fMRI)

FMRI was collected using repeated single-shot echo-planar imaging with the following characteristics: TE=30 ms, FA=90°, in-plane resolution=2*2 mm^2, 75 slices acquired in an ascending and interleaved order, slice thickness=2 mm and TR=1700 ms (ARC=2, HB=3). We acquired one 10-min resting state fMRI sequence with eyes open.

MR Spectroscopy (MRS)

MRS measurements of glutamate was performed in each of the two large (4 x 4 x 3 cm^2 = 48 cc) volumes of interest, both placed medially one encompassing supplementary motor areas (SMA), and one encompassing the Posterior Cingulate Cortex (PCC) shown in Figure 2.7.

Prior to MRS acquisition, automated high-order shimming was performed to improve the magnetic field homogeneity within the volume of interest. Two successive localized MRS acquisitions would then be collected from each region, each one using an identical Point REsolved SpectroScopy (PRESS) Sequence with the following sequence parameters: TR/TE=2000/270ms 35ms, 152 averages, 4096 spectral points, 4500 Hz spectral width, CHEmical Shift Selective saturation (CHESS) water suppression, and 8 step phase cycling. Each acquisition had a duration of approximately 10 minutes. The echo time was chosen to enable detection of glutamate, since at this echo time the glutamate signal is maximally upright, and the overlapping macromolecules are fully suppressed due to T2 relaxation (since macromolecules have a shorter T2 than glutamate).

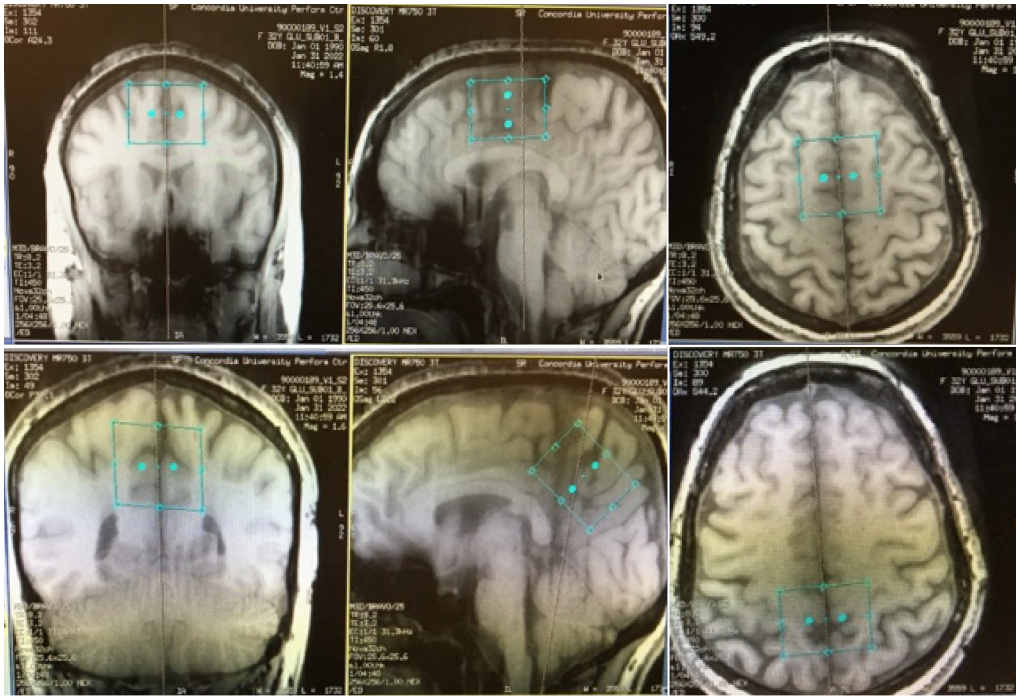

Figure 2.7: MRS single voxel positioning; First row shows positioning the voxel on the SMA area and second row shows it for the PCC area in coronal, sagittal and transverse planes respectively.

2.2.2 Electroencephalography (EEG)

EEG setup consisted of installation of 32 scalp electrodes placed on the scalp using EEG free electrodes. The location of the scalp electrodes were determined based on the international 10-20 system of placing the electrodes. Electrodes were attached to the scalp using a clinical adhesive called collodion, which allows prolonged recordings without the EEG paste being dried or without the electrodes moving throughout the day of acquisition. An abrasive gel was used to keep the scalp-electrode resistance below 5KOhm at all times.

EEG was recorded using an MR compatible Brainamp amplifier (Brainamp MR Plus, Brain Products GmbH, Gilching, Germany). FCz (fronto-central electrode) was considered as the reference electrode. Also, a bipolar electrocardiogram (ECG) was acquired for balistocardiogram (BCG) removal using a bipolar MR compatible Brainamp amplifier (Brainamp ExG MR, Brain Products GmbH). EEG data was sampled inside the MRI scanner at 5 KHz with 500 uV resolution. Hardware filters were set to a high-pass filter at 0.0159 Hz and low-pass filtered at 250 Hz and data was sent to the MRI control room via the fiber optic cables where a laptop with BrainVision Recorder

Software Version v1.03 (BrainVision Recorder, Version 1.03, Brain Products GmbH) and the Brain Product sync box (Brain Products GmbH) were installed for synchronizing the scanner clock with EEG sampling and recording.

To minimize the head movement in the scanner and to avoid movement artifacts, subjects' head were kept immobilized inside the head coil using vacuum pads. EEG cables inside the scanner were fixed using sand bags to minimize the effect of scanner vibrations.

2.2.3 Cortisol and Melatonin Measurement

All organisms are exposed to light-dark and temperature cycles as a result of the earth rotation around its axis and therefore they developed an internal clock known as circadian clock. Circadian rhythm will allow them to predict the daily changes of environment. The circadian pacemaker in the brain is the molecular oscillators in the suprachiasmatic nucleus (SCN) in the hypothalamus which create an approximately 24-hour periodicity for the circadian cycle. The endocrine biomarkers of circadian rhythm driven by SCN are melatonin, cortisol and core body temperature [41].

In this study, we collected each participant's saliva to measure their melatonin and cortisol levels. For melatonin, 9 samples were collected at 8:00, 13:00, 17:00, 18:00, 19:00, 20:00, 21:00, 22:00, 8:00 (day after) and for cortisol 6 samples were measured at 9:00, 11:00, 13:00, 17:00, 19:00, 8:00 (day after) during waking hours and 40 minutes post-awakening.

2.3 Screening and Recruiting Participants

2.3.1 Participants

In this study, around 30 people were screened for the inclusion/exclusion criteria of the study through a participants' questionnaire with 35 questions designed in Microsoft Form (Figure 2.8). 6 healthy right-handed young adults (age 18 to 35, 1 female) were recruited. Once selected, they were presented about the duration and the general view of the protocol that they were going to experience.

All participants signed a written informed consent approved by the Central Research Committee of the Minister of Health and Social Services of Quebec (Comité central d'éthique de la recherche

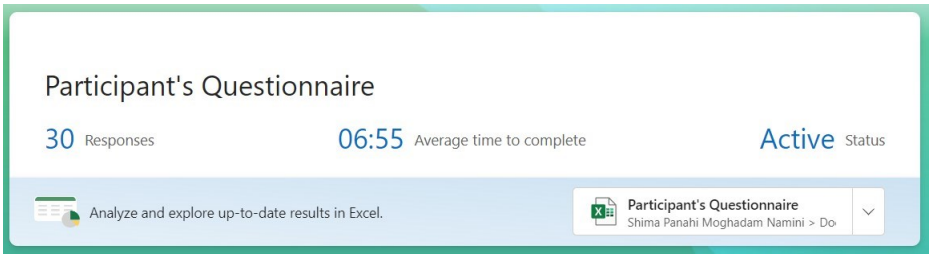

Figure 2.8: Participants' Questionnaire Summary

(CCER) du ministre de la santé et des services sociaux du Québec) and received monetary compensation upon completion of the study. In data analysis, the female subject was removed due to having noisy data. The data of these subjects was to test the feasibility of the study.

2.3.2 Participants' Recruiting Criteria

Inclusion Criteria:

- Healthy
- Right-handed
- Adults age between 18 to 35 years old
- Able to use a keyboard for typing
- Good sleepers
- Meet the safety guidelines of the 3T MRI scanning policy

Exclusion Criteria:

- Having a medical condition (sleep disorders, mental disorders, neuro-psychiatric history, depression, anxiety, etc.)
- Left-handed
- Younger than 18 or older than 35 years old

- Musician or video gamer (current or in the past) or highly skilled typist or not able to use a keyboard for typing
- Having worked on night shifts or having traveled through a different time zone during the last three months
- Having uncorrected visual impairment
- Drinking alcohol or caffeinated drinks excessively (more than 3 times per day), using illicit drugs, smoking, taking medications
- Not meeting the safety guidelines of 3T MRI scanning policy (such as being claustrophobic, having pacemaker or metal fragments in body, metal prosthesis, heart/vascular clip, prosthetic valve, pregnancy)
- Having exams between the two sessions of the experiment
- Having difficulty with their sleep (assessed using a questionnaire for monitoring their Insomnia Severity Index)

2.3.3 Location and Duration of the Study

This study was implemented in Imaging and Physical Suites and Sleep Lab at Perform Center (presently named School of Health), Concordia University. Each participant had to attend the study in two visits for a total duration of 42 hours. Each visit was two to three weeks apart. The pilot phase of the study and troubleshooting occurred during 2022 and data collection during 2023.

2.4 Softwares Utilized in the Analysis

The softwares that were used in this particular thesis work include BrainVision Analyzer Software Version 2.2.1. (Brain Products, GmbH) for preprocessing EEG data, EEGLAB [42] Software Version 2023.1 for further denoising of EEG data, Matlab Software Version R2019a for extracting the power spectrum density of EEG signals using the EEGlab functions and R Software [43] for implementing the linear mixed model which are explained further in Chapter 3.

Chapter 3

Implementation, Data Preprocessing and Analysis

3.1 Implementation of the Protocol

When it comes to practice, each study has its own constraints. And based on the constraints, we need to modify things to be able to adjust and optimize the situation to get the best results. In this study due to the existing limitations, we had to use a special set of free electrodes and measure the EEG 10-20 system in a fast way which is discussed below. I will also discuss about collodion application process, recording BCG and EEG-fMRI setup in this study.

3.1.1 A Special Set of EEG Free Electrodes for the MRI Coil

Normally, an MRI coil has a whole on top of the coil along the Z axis for exiting the EEG cables from the center. In our case at Perform Center, the specific MRI coil that we were willing to use for its MRS specifications did not offer this capability for simultaneous acquisition with EEG. Therefore, we had to use the eye wholes of the coil to exit the EEG cables. The length of the current EEG cables that we had at the time were standard; when we tested them, the connectors which had metal parts would remain inside the coil (Figure 3.1) and their magnetisation would create inhomogeneity in the field map and cause artifacts on the MR images.

This meant we needed longer EEG cables to have the connectors out of the coil and exit from

Figure 3.1: Length of the old set of EEG free electrodes (on the left). Metal connectors shown with the red arrows (center). In the coil, eye whole is shown with the yellow arrow and the metal connector inside the coil is pointed with red arrow (on the right) indicating the insufficient length of EEG cables which would cause the connectors remain inside the coil and create artifact on MR Images.

the Z axis of the scanner. Therefore, we did the necessary measurements on a phantom and ordered a set of 32 channel EEG free electrodes from McGill University that would be convenient for the coil that we had at Perform Center.

Testing the New Electrodes

We tested the new set of free electrodes in saline (Figure 3.2) to check for the impedance of the electrodes and replaced the electrodes showing a high impedance.

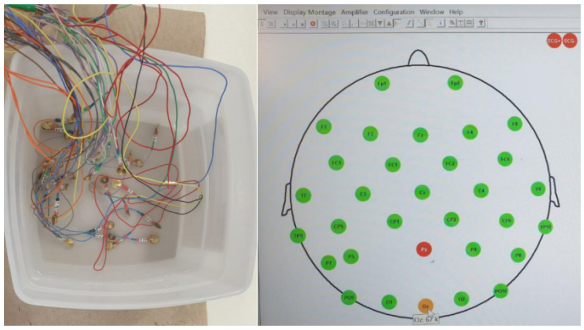

Figure 3.2: New set of electrodes in saline (on the left) and their impedance map (on the right). Electrodes showing a high impedance were replaced.

We also checked the new electrodes in the MRI scanner on a watermelon phantom to check

the noise immunity of the system. Watermelon has a conductive surface and allows for keeping the impedance below 5KOhm at its contact surface with the electrodes which is necessary for protecting the amplifiers from a high voltage induced by MRI and to control for heating [44].

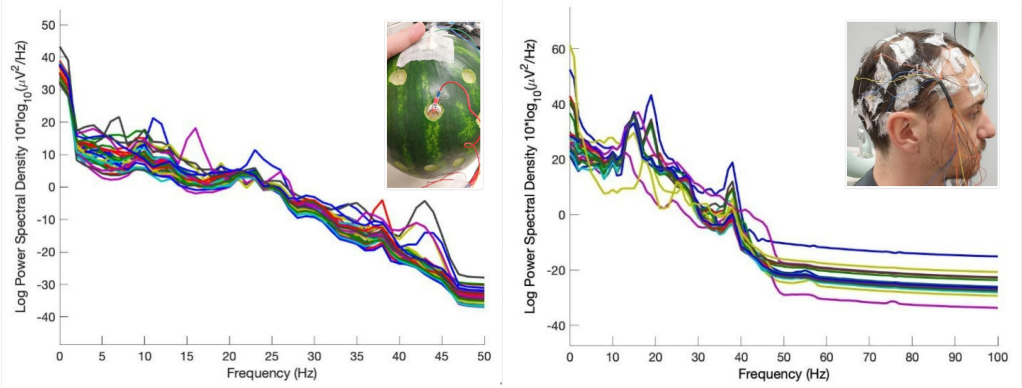

Figure 3.3: Testing the new set of free electrodes on a watermelon phantom and a pilot on human; PSD of the collected signals from the phantom without any noise (left) and PSD of the acquired EEG from a human indicating the presence of noise (right).

The watermelon skin was removed where applying the electrodes, and electrodes were installed using conductive paste. The power spectrum density (PSD) of the acquired signals in the scanner didn't imply on the existence of any unusual noise (Figure 3.3 left).

3.1.2 Measuring the Standard 10-20 System Faster!

In this study, each participant would arrive at 7:00 am and we had a short amount of time to prepare him for the data acquisition. Participant had to change their clothing upon arrival and meanwhile we would prepare a sit for him with the necessary equipment for vacuuming the air (due to the usage of collodion) and tools for installing the electrodes such as alcohol, swab, abrasive gel, conductive paste, gauze, collodion and collodion remover, etc. The installation of electrodes would begin at 7:30 am and the first acquisition was at 9:30; therefore, we had less than 2hrs to measure the standard 10-20 system, install the free electrodes with having the impedance below the 5KOhm, prepare the EEG equipment in the MRI room for simultaneous EEG-fMRI acquisition and have the participant ready in the scanner on time.

The International 10-20 System

The international 10-20 system (Figure 3.4) allows for a uniform measurement of participants' head for placing the EEG electrodes. In this system, four reference points are considered for measuring the scalp; the nasion, the inion and the two preaurical points. From these points the transverse and median planes are considered to measure the location of each electrode by dividing the intervals into %10 and %20 distances [45].

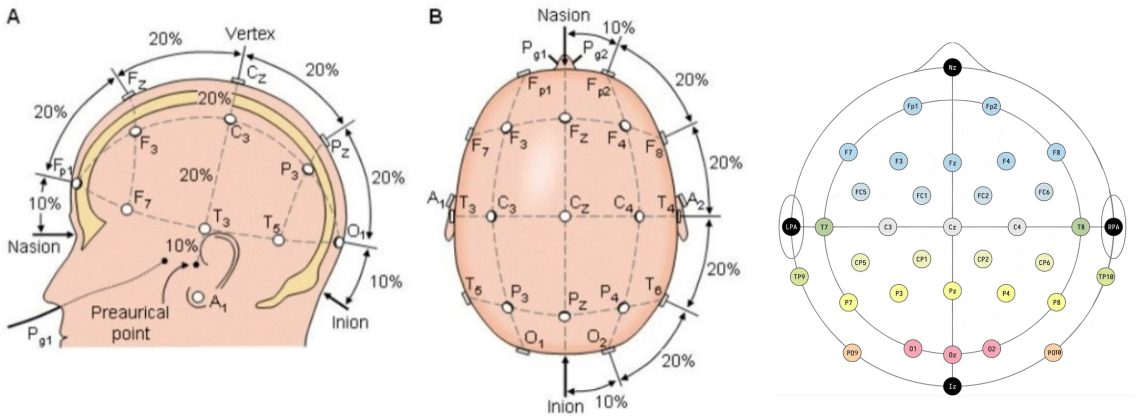

Figure 3.4: The International 10-20 System [45] (on the left and center) and EEG 32 channel map modified for this thesis from here (on the right).

Fast Measurement of the 10-20 System

Having a short amount of time for preparation before the first scan starts, I proposed to measure the 10-20 system using an EEG cap (Figure 3.5). To check the precision of this method, we tested the measurements on one pilot subject who shaved his head for this purpose. First, we measured the 10-20 system on his head (Figure 3.6 red crosses). Second, we used the reference points (nasion, inion and preaurical points) to align an EEG cap with the head correctly and marked the points using the cap (Figure 3.6 green dots). Eventually, we measured the differences between the two measurements which on average was less than 7mm. Considering the spatial resolution of EEG, this was completely acceptable. Therefore, we reduced the measurement time to 5-10 minutes and saved time for installing the electrodes and other preparations.

Figure 3.5: Marking the electrode positions using an EEG cap. The cap was aligned with the 10-20 reference points.

Figure 3.6: The standard 10-20 system measured manually (red crosses) and marked using an EEG cap (green dots). The difference between the two methods of measurement was less than 7mm.

3.1.3 The Collodion Application Process

Based on the American Clinical Neurophysiology Society Guidelines [46], EEG electrodes can be attached to the scalp using paste or collodion which is a strong and durable clinical glue used in many hospitals for prolonged EEG collection as it can withstand movements specially during sleep. It is water resistant and dries out slowly when exposed to air due to the evaporation of ethyl ether [47].

At the Physiology Suite at Perform Center, while installing the electrodes we used the compressed air system with high pressure air to speed up gluing and at the same time a fume extractor to vacuum the ethyl ether evaporation with its strong odor for keeping the ventilation at a proper level. Since collodion is flammable, we also had to take precautions about storing and disposing it for its chemicals. At the end of each study, all the chemical wastes of collodion were collected in specific chemical waste bins at Perform for proper disposal.

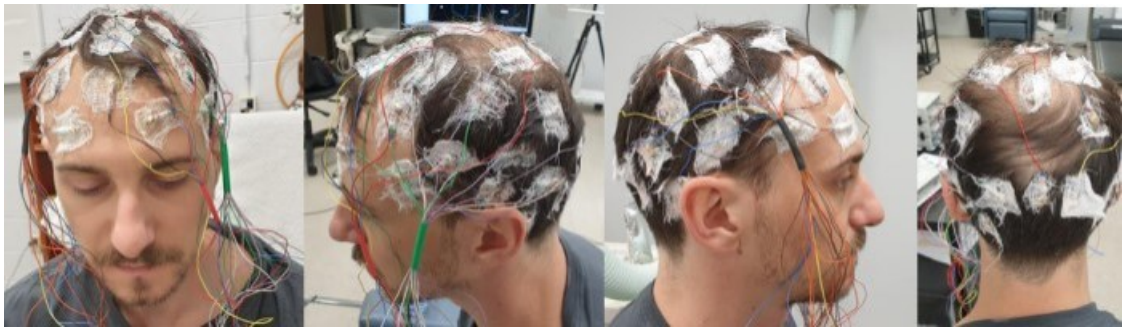

Figure 3.7: Free electrodes installed with collodion

Participants were protected from the glue drops using a towel around their neck and shoulder. Also, when applying the glue for frontal electrodes, they were asked to cover their face and specially eyes with a towel until the application was finished to keep them safe.

For each participant, the hair was parted and the scalp was cleaned using alcohol and a cotton-tipped stick drenched in abrasive gel. The electrode was placed on the cleaned scalp using the EEG conductive paste. A square of gauze (2–3 cm) was placed on the electrode, the collodion was applied and dried using the compressed air. Figure 3.7 shows the installation of free electrodes using collodion for a pilot subject.

At the end of each visit, the collodion was removed using collodion remover and participants were allowed to further wash their hair with a regular shampoo and dry their hair.

The use of collodion made it possible to apply the electrodes only once during each visit and avoid the re-installation before each scan which would make the implementation of the protocol intolerable for the participants and complicated for the staff.

3.1.4 Recording the Ballistocardiogram

One of the challenges of simultaneous EEG-fMRI is the artifacts caused by movement in the scanner. Ballistocardiogram (BCG) is one of the major artifacts in EEG-fMRI caused by the micro-movements of heartbeat pulsations. BCG is a non-stationary signal which varies electrode by electrode for each subject [48] and it is very crucial to record it properly for future preprocessing and artifact removal from the EEG data.

Cardiac axis is considered as the net direction of electrical activity during depolarization and

can be determined using the 6 limb leads (I, II, III, aVR, aVL, aVF) which look at the heart from different angles in a vertical plane. Here the purpose is just to record the R-peaks with a good resolution in the scanner. In the current study, we used lead III for detecting the R-peaks.

3.1.5 EEG-fMRI Setup

Setup in the MRI Room

Figure 3.8 provides a schematic of the EEG setup in the MRI room and MRI control room [49] and below, the details are explained.

- The EEG equipment in the MRI room included:

(1) A PowerPack (MR rechargeable battery, Brain Products GmbH, Gilching, Germany)

(2) An MR compatible Brainamp Amplifier (Brainamp MR Plus, Brain Products GmbH, Gilching, Germany) for recording EEG

(3) A bipolar MR compatible Brainamp Amplifier (Brainamp ExG MR, Brain Products GmbH, Gilching, Germany) for recording BCG

- The outputs from the MRI room included:

(1) From the BrainAmp MR amplifiers, EEG and BCG signals were directed out to the control room using the fiber optic cables (FOC) and reached the USB2 Adaptor input.

(2) From the MR scanner, the MRI Master Clock signal was directed out to the control room where we had the SyncBox interface connected to the SyncBox Main Unit which was connected to the USB2 Adapter input and to the laptop separately using a USB cable.

Setup in the MRI Control Room

- The EEG equipment in the MRI control room included:

(1) USB2 Adaptor: a USB interface to connect the amplifiers to the recording laptop

(2) Syncbox: a tool which synchronizes the clock driving the MRI's gradient switching system with the clock of EEG recording system

(3) Laptop with BrainVision Recorder: a software for controlling the amplifiers, displays and saves the incoming EEG/BCG signals and the trigger information

- Recording the signals in the control room

  The output of fiber optic cables from the amplifiers in the MRI room and the output of SyncBox would connect to the input of USB2 Adaptor and the output of USB2 Adaptor would connect to the laptop where we had the BrainVision Recorder for visualization and recording of EEG and BCG signals.

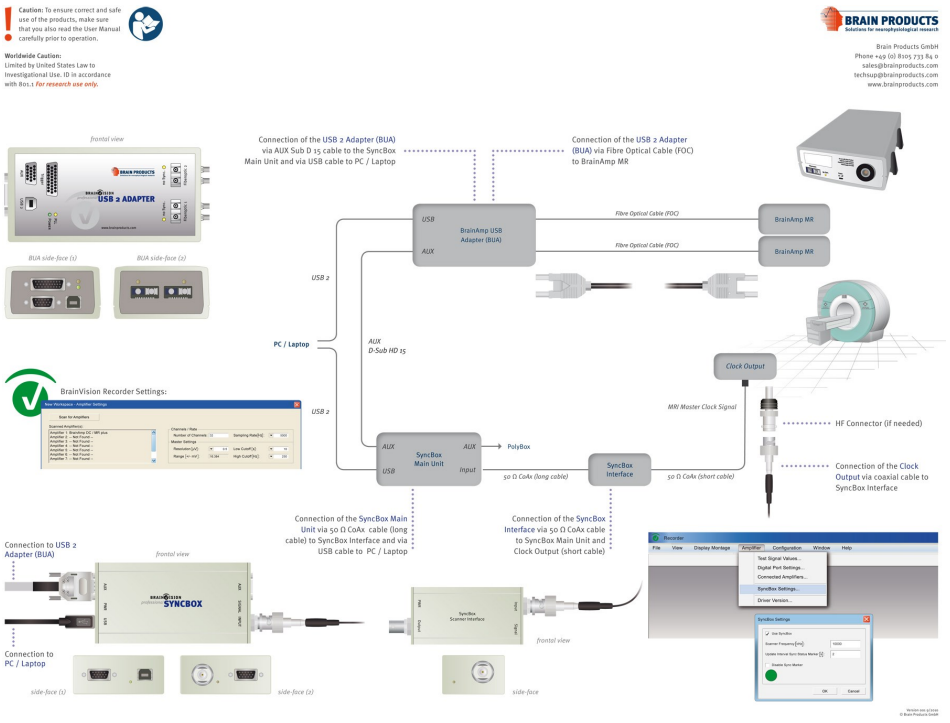

Figure 3.8: EEG-fMRI setup in the MRI room and MRI control room [49].

3.2 Preprocessing the EEG Signals

3.2.1 EEG-fMRI and Its Artifacts

When EEG is collected simultaneous with fMRI, it is subjected to different artifacts such as the gradient artifact (GA), the ballistocardiogram (BCG), motion artifacts and other ambient noise [48, 50]. Below, each of this artifacts and how they are removed from our EEG data are explained.

Gradient Artifact

The gradient artifact (GA, shown in Figure 3.9 a) which occurs due to the magnetic field gradient of fMRI, induces current in EEG electrodes and can create a large artifact on the EEG data. This artifact is assumed to be periodic happening during each TR and can be removed by template methods. To collect the GA artifact accurately, a synchronization hardware device is used to synchronize the EEG recordings with the MRI clock.

The earliest and best template method developed to remove GA was the average artifact subtraction (AAS) method. AAS method can leave the EEG data with residuals of GA since the EEG data can experience non-stationarities (due to the head motion, BCG, etc.) [50].

Ballistocardiogram Artifact

BCG artifacts occur by cardiac motions and scalp pulsations and since the amplitude is larger than EEG, it can confound with the EEG signal. Recording the chest ECG during EEG-fMRI gives an estimation of BCG which can help removal of BCG artifact. This artifact can also be removed by the template methods [48, 50].

Motion Artifact

According to Faraday's law, the subject's motion under the magnetic field can induce current in the electrodes and thus produces motion artifact on the signals of interest [51].

Ambient Noise

EEG in the scanner is also prone to environmental noise as it can interfere with vibrations of the helium pump for cooling the scanner, line noise, ventilation and light present in the scanner or the room [50, 52]. In the current experiment, helium pump was off while recording EEG-fMRI.

3.2.2 Preprocessing: Removing the Gradient Artifact

For scanner artifact correction, the BrainVision Analyzer Software Version 2.2.1. (Brain Products, GmbH) was employed. Within this software the MR Correction transform was used to detect and remove the gradient artifact from the EEG signal. This toolbox uses the Average Artifact Subtraction (AAS) method introduced in [53]. The method takes an average over the intervals of EEG signal interfered with the scanner's magnetic field gradient. The averaging reduces the contribution of the EEG signal to the output curve and produces a template of the gradient artifact for correcting it's interference. The template is then subtracted from the original data in each TR interval allowing for the elimination of the GA. Since the EEG data is also contaminated by other types of artifacts which makes it non-stationary, this method might not be able to remove the scanner artifact completely. Thus, further filtering from the same toolbox will be used to correct the data. Figure 3.9 shows the GA removal for EEG of one subject.

TR markers

In this study, the BrainVision SyncBox was used to synchronize the MRI Master clock with the EEG amplifier. Therefore, the TR start points or markers are recorded. Having the TR marker will allow for the precise detection of each TR interval for extracting the GA artifact template and will also help to avoid the drifts of the TR in relation to the sampling rate.

EEG Post Correction

After the GA removal, post correction was also done using the MR Correction transform. The sampling rate was reduced to 250 Hz and the data was low-pass filtered using an FIR filter with cut-off frequency of 55 Hz.

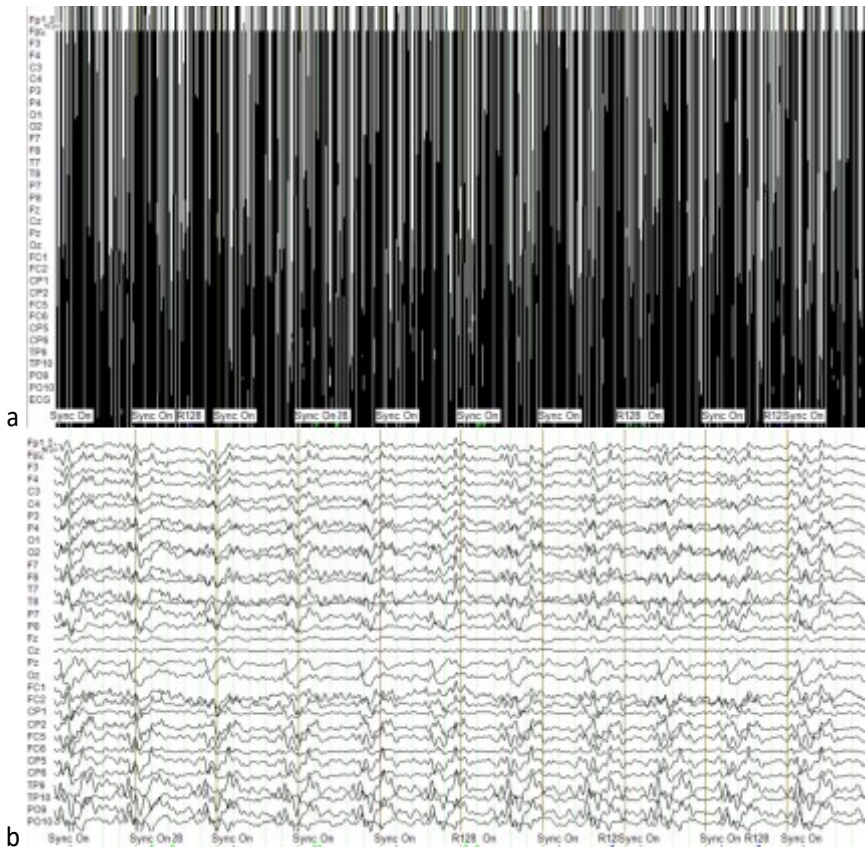

Figure 3.9: a) 10 sec of EEG data contaminated by the Gradient Artifact b) 10 sec of EEG data after removing GA in BrainVision Analyzer

3.2.3 Removing the Ballistocardiogram Artifact

After GA elimination, removing the BCG artifact was also done in BrainVision Analyzer using the CB Correction transform. In this stage, the recorded BCG signals were searched for ECG episodes using the semiautomatic mode. The software detected each pulse automatically, but would allow to adjust the position of each pulse manually in case they were placed wrongly or if some of the pulses were missed by the software. Therefore, the start point of all the pulses were checked and adjusted manually and the BCG R-peak markers were then generated based on the manual correction of the pulse positions. Based on the defined recurring attribute of pulse beats and the R-peak markers, the correction of BCG artifact were then done using the template averaging process defined in the software. The calculated average curve was subtracted from the EEG signal for each BCG episode. A sample result is shown in Figure 3.10.

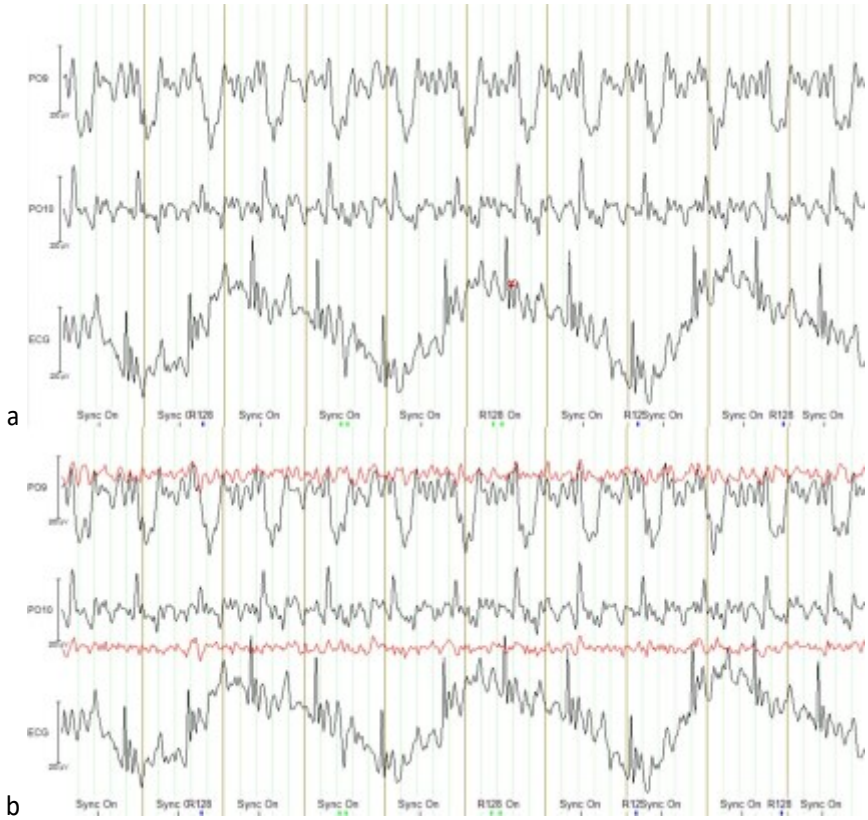

Figure 3.10: a) 10 sec of BCG (ECG channel) signal as well as the contaminated EEG channels b) The red overlays shows 10 sec of EEG data after removing BCG artifact in BrainVision Analyzer

3.2.4 Further Denoising with Independent Component Analysis

Apart from the mentioned artifacts, EEG can also be contaminated with the motion artifacts, eye blinks, muscle artifact, the residuals of GA and BCG, ambient noise and residuals of line noise.

Independent Component Analysis (ICA) is one of the methods that allows for decomposition of EEG into the original sources which tend to produce the EEG activity at the scalp level [54]. When the data is contaminated by different artifact sources, ICA can also be used to approximately separate the noise from the signal as an independent component [55]. In the current study, EEGLAB [42] Software Version 2023.1 was recruited for ICA decomposition and the IClabel Version 1.6 plugin was used for automatic classification of noise and labeling each component into the known categories.

In EEGLAB, the data was first visually inspected for bad channels and if there were any, they were interpolated using the Spherical method. The signals were then re-referenced to the average

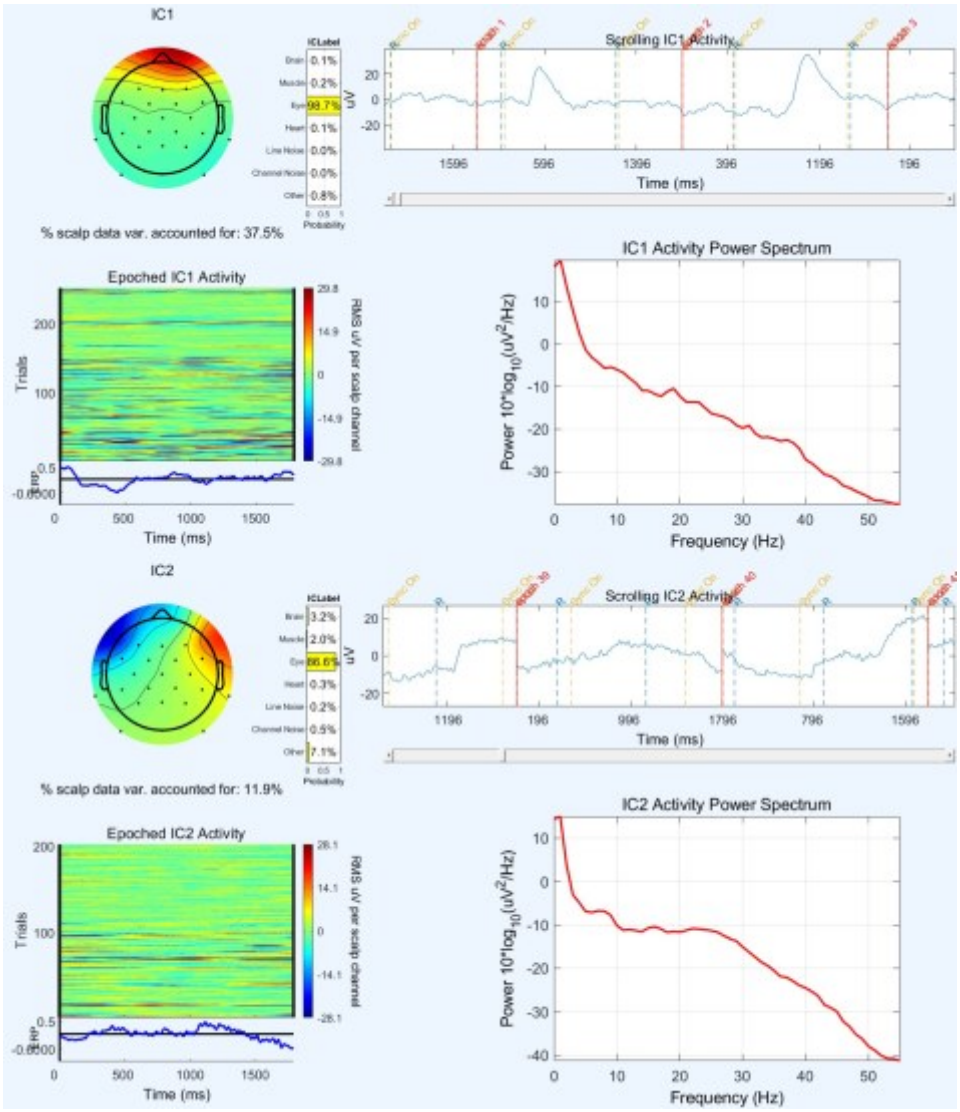

Figure 3.11: Eye blink components captured by ICA decomposition in EEGLAB. a) Vertical eye movement b) Horizontal eye movement

and high passed filtered at 0.5 Hz. Before running the ICA, the data was visually inspected for motion artifacts and bad segments were removed manually. In EEGLAB, the default ICA method Infomax Runica [42] was used for decomposition of EEG siganls.

Eye Components

Eye components explain the vertical and horizontal eye movements and it mostly contains frequencies below 5Hz. Figure 3.11 (a) shows the scalp topography for vertical eye movement and

Figure 3.11 (b) shows the scalp topography for horizontal eye movement.

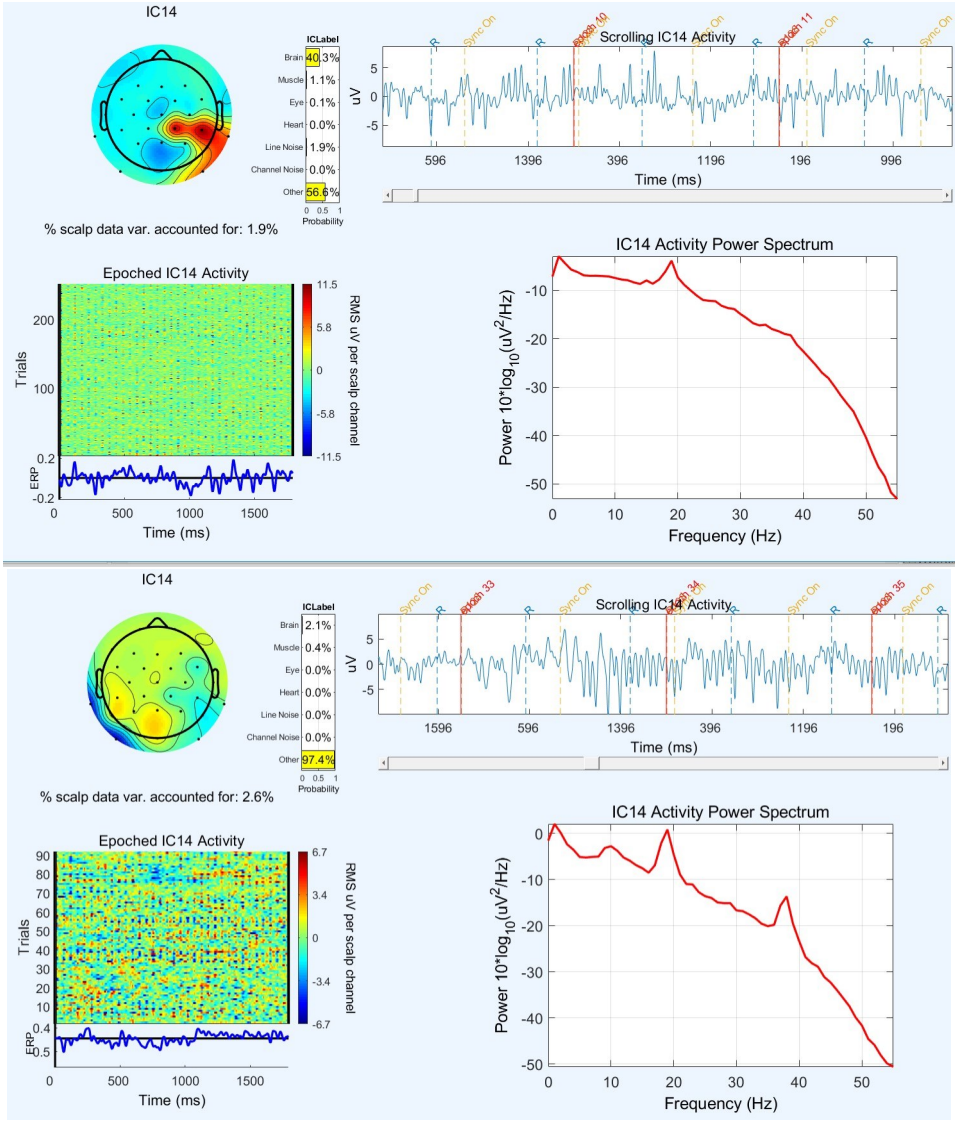

Figure 3.12: Gradient artifact residuals captured by ICA decomposition in EEGLAB for two different subjects

Components with GA Residuals

The power spectrum of the EEG signal can be overlapped by the harmonics of repetition frequency and volume repetition frequency from the fMRI sequence and therefore, the harmonics of gradient artifact can be seen on the EEG power spectrum [56].

Although the GA was removed from the EEG signals with AAS method, the AAS method might

not be completely effective due to the reason that the signal is interfered with different noise sources at the same time and might not necessarily be stationary. Therefore, when we run the ICA, we can see components with power spectrum density containing frequency of approximately 19Hz (related to MRI sequence parameters) and it's harmonics representing the residuals of the GA. This is shown in Figure 3.12.

Components with Heart Beat Residuals

Same as the GA, BCG artifact residuals can also remain after the average template subtraction technique. Therefore, ICA decomposition can also extract components that contains the pulse residuals. Figure 3.13 shows an example of this case; In this subject, BCG artifact was not removed properly in the template subtraction method due to having a bad ECG channel in the scanner and therefore, it is extracted with ICA.

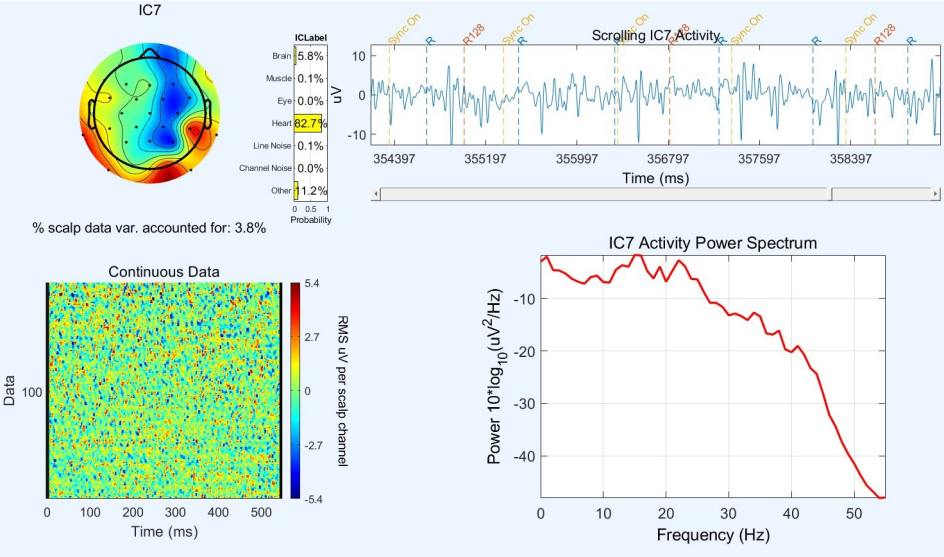

Figure 3.13: BCG artifact residuals captured by ICA decomposition in EEGLAB

3.3 Processing the EEG Signals

3.3.1 Extracting the EEG Power Spectrum Density

After noise removal, the EEG signals were transferred to Matlab Software Version R2019a for analysis. The power spectrum density (PSD) of the signals from each electrode was extracted using the EEGLAB [42] Spectopo function using the Pwelch method. For calculating PSD in each frequency bin, a 2-second window with %75 overlap was considered; For each window, the method took advantage of zero padding and tapering using a hamming window to avoid Gibbs phenomena and eventually averaged over the entire segments. The values were normalized by a logarithmic base 10 transform. Then the average of PSD values was estimated over each conventional band, that is, delta (1-4Hz), theta (4-8Hz), alpha (8-13Hz), beta (13-30Hz) and low gamma (30-55Hz) bands illustrated in Figure 3.14. Eventually, the PSD values for each band were introduced to a Linear Mixed Effect Model for further analysis.

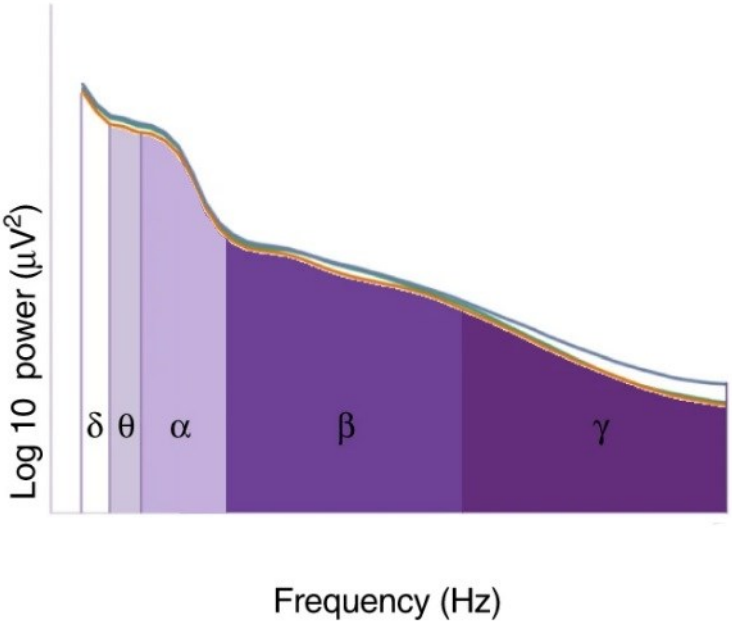

Figure 3.14: Schematic of PSD for each frequency band adapted from [57]

3.4 Statistical Analysis

3.4.1 Group-Level Estimations Using Linear Mixed Effect Models

Linear Mixed Models (LMMs) are statistical models that combine fixed and random effects in a linear predictor expression to represent the data behavior. From the prediction, we can assess the conditional mean of the response [43]. In this study, two Linear Mixed Effect models were implemented in R Software [43] to test the hypothesis at a group-level. For both models, subjects are considered as the random effects.

We used the first Linear Mixed Model (LMM1) to estimate the group-level contrasts in EEG data to test if there are task-related neuronal activity in EEG. The predictors for this model were the averaged PSD intercepts for each condition.

As mentioned before, in this study, participants were in one of the following conditions before they went to the MRI scanner:

(1) Rest (R): participants were resting

(2) Control (C): participants were performing the Control task

(3) MSL (M): participants were performing the MSL task

For LMM1, we averaged the repetition of each condition on the Control day and the MSL day and considered the following contrasts:

- M vs C
- M vs R
- C vs R

We used the second model, LMM2, to estimate whether there is any correlation between the longitudinal behavior of the PSD and the glutamate. The values were normalized so that the slope of the fitted line can be interpreted as the correlation.

Figure 3.15 shows an illustration of the two models.

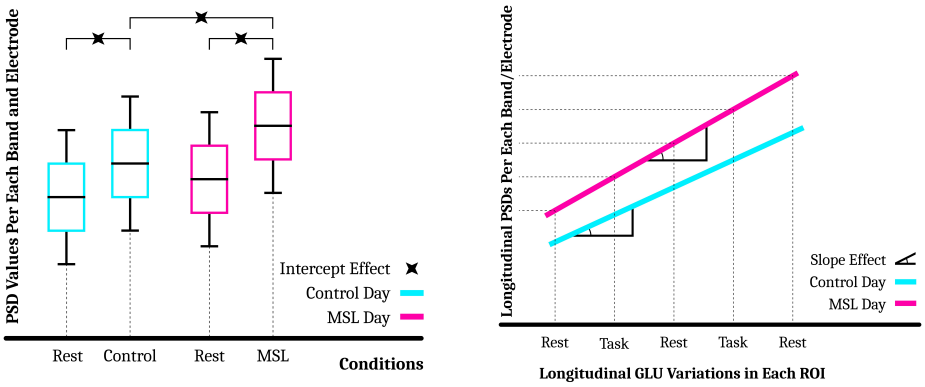

Figure 3.15: Schematic of the two Linear Mixed Models; LMM1 on the left and LMM2 on the right.

Chapter 4

Results

In this chapter, the results of group-level analysis using the implementation of the two Linear Mixed Models (LMM) are presented. LMM1 describes the power spectrum density (PSD) of the EEG in three different contrasts. LMM2, explains the longitudinal behavior of PSD as a function of glutamate concentrations (GLU, acquired by MRS[1]. In each section, the observed result of each model is summarized in a table. In the table, each electrode is assigned to the closest brain area shown as a small box on the electrodes in Figures 4.1, 4.2 and 4.3. Of course, source reconstruction would be needed if we want to locate the exact source of electrical activity. It is also important to mention that the data is collected while the participants are resting in the scanner the whole time. In task-related (MSL or Control) sessions, the EEG data was acquired around 15^{+} minutes after the task (including the participant preparation time in the MRI scanner and 5 min T1 acquisition before the EEG-fMRI collection starts). For the Glu levels, this time delay is 30^{+} minutes as it was collected after 10 minutes of EEG-fMRI collection.

4.1 Group-Level Estimations of EEG in Different Contrasts

In LMM1, the PSD behavior per each band and each electrode is estimated under three different contrasts: MSL vs Control, MSL vs Rest, and Control vs Rest which is presented below.

[1]The MRS data of this project was processed in a thesis work by another student [58]

4.1.1 EEG Variations in MSL vs. Control Sessions

Table 4.1 shows the results of the LMM1 for the M (MSL task) vs C (Control task) contrast. In this model the two M sessions on the MSL day were used to compare with the two C sessions on the Control day. For an illustration of the results please refer to Figure 4.1.

M vs C Contrast: During the MSL task (M) participants were experiencing motor sequence learning with the finger-tapping movements. During the Control task (C) participants were only experiencing finger-tapping movements with no learning. Therefore, by contrasting M vs C, we are expecting to eliminate the impact of finger-tapping movements and detect only the neuronal activity related to motor sequence learning.

The LMM1 Results for M vs C shows statistically significant neuronal representations in the task-related ROIs. We can see the EEG electrodes FC2 and Cz located on the SMA region which is a key region in sequence processing [34]. We can also see the EEG electrode CP2 located on the Primary Motor Cortex (M1) which was shown to have contribution in motor skill learning [12].

The manifestation of these task-related memory representations contralateral to the non-dominant hand of the subjects is what we expected from the paradigm which is also in line with the literature in fMRI [5, 11, 12], MRS [20] and EEG [59] studies.

ROI	Channel	Band	Contrast	Standard Error	p-value<0.05
SMA	FC2	low gamma	4.231	1.654	0.041
SMA	Cz	low gamma	4.616	1.803	0.041
M1	CP2	low gamma	4.316	1.705	0.044

Table 4.1: Results of the Linear Mixed Model (LMM1) for the contrast M vs C

Task-related Band Specific Oscillations: The captured neuronal representations were significant in low gamma band (30-55 Hz). This shows that task-related motor activity, in comparison with the Control condition, induced an increase in the power density in low gamma band. Gamma band has been constantly observed to be induced during movement and appears to play a key role in learning [60, 61].

4.1.2 EEG Variations on MSL Day, MSL vs Rest Sessions

Table 4.2 shows the results of the LMM1 for the M (MSL task) vs R (Rest) contrast on the MSL day. In this model the two M sessions were used to compare with the three R sessions on MSL day. For an illustration of the results please refer to Figure 4.1.

M vs R Contrast: During the MSL task (M) participant was experiencing motor sequence learning with the finger-tapping movements. Rest (R) sessions means that the participant was resting (absence of performing any task) before going to the MRI scanner.

For the MSL day, the two MSL sessions were considered to be compared with the three rest sessions before the night acquisition for the contrast; the session recorded after sleep (the day after) as the 6th acquisition were excluded from this analysis as sleep has an important impact on neuronal regulations [19]. By contrasting M vs R, we are expecting to see the impact of finger-tapping movement as well as the neuronal representations of motor sequence learning.

The LMM1 Results for M vs R on MSL Day shows statistically significant neuronal representations in the task-related ROIs. We can see the EEG electrodes FC2 located on the SMA, and CP2 located on the M1 which were already seen when we contrasted M vs C indicating that these regions are associated with performing the motor sequence learning task. In this contrast M vs R, we are including the impact of finger-taping movements and the model shows a significant neuronal activity in EEG electrodes C4 and FC6 located on Premotor Cortex Dorsal (PMd) and Ventral (PMv) which was shown to modulate Primary Sensory (S1) cortex in human voluntary movements in an fMRI and an Electrocorticography (ECoG) study [62, 63]. FC6 (with delta band) seems to be on the neuronal region associated with fingers and their movement as it can also be seen in table 4.3 when contrasting C vs R on Control Day.

Task-related Band Specific Oscillations: The captured neuronal representations were significant in delta (1-4 Hz), theta (4-8 Hz), beta (13-30 Hz), low gamma (30-55 Hz) and overall bands (0.5-55 Hz) for the motor cortical regions. The results show that task-related motor activity, in comparison with the rest condition, induced an increase in the power density in beta, low gamma and overall bands in SMA and PMd and only low gamma band in M1 after the task. Here, when we take into account the finger-tapping movements effect, we can see the manifestation of lower bands

ROI	Channel	Band	Contrast	Standard Error	p-value<0.05
SMA	FC2	beta	2.639	0.998	0.016
SMA	FC2	lowgamma	2.622	1.043	0.021
SMA	FC2	all	434.241	181.579	0.027
M1	CP2	lowgamma	3.12	1.141	0.013
PMd	C4	beta	2.517	0.977	0.018
PMd	C4	low gamma	2.977	1.002	0.008
PMd	C4	all	474.968	177.314	0.015
PMv	FC6	delta	2.605	1.096	0.028
PMv	FC6	theta	2.543	1.082	0.03
Visual	O2	theta	1.759	0.771	0.034

Table 4.2: Results of the Linear Mixed Model (LMM1) for the contrast M vs R on MSL day

delta and theta in the PMv area which is a region responsible for the modulation of human voluntary movements [63]. Delta and theta bands were shown to manifest in fronto-central regions in finger-tapping paradigms known to be related to motor decision making [64], and beta band which was shown to increase in motor cortical regions under MSL in PM and SMA [59].

4.1.3 EEG Variations on Control Day, Control vs Rest Sessions

Table 4.3 shows the results of the LMM1 for the C (Control task) vs R (Rest) contrast on Control day. In this model the two C sessions were used to compare with the three R sessions on Control day. For an illustration of the results please refer to Figure 4.1.

C vs R Contrast: During the Control task (C) participants were only engaged in the finger-tapping movements without any specific experience learning. Rest (R) sessions means that the participant was resting (absence of performing any task) before going to the MRI scanner. By contrasting C vs R, we are expecting to see the electrical activity related to the finger-tapping movement.

The LMM1 Results for C vs R on Control Day shows statistically significant neuronal representations for finger-tapping movement manifesting on the EEG electrode FC6 located on the PM area, which was also captured by the LMM1 model when contrasting M vs R but not M vs C on MSL day, indicating the neuronal representations for the modulation of human voluntary movement by the PMv area [62, 63].

ROI	Channel	Band	Contrast	Standard Error	p-value<0.05
PMv	FC6	delta	2.713	0.946	0.01
Visual	O1	delta	3.112	0.995	0.006
	F8	delta	2.629	0.84	0.006
	P8	delta	2.256	0.755	0.008
	P7	delta	2.558	1.009	0.02
	T8	delta	3.123	1.047	0.008
	T7	delta	2.348	1.056	0.039
	TP10	delta	3.141	0.898	0.002
	TP9	delta	3.614	1.069	0.003
	PO9	delta	2.801	0.935	0.007

Table 4.3: Results of the Linear Mixed Model (LMM1) for the contrast C vs R on Control day

Task-related Band Specific Oscillations: The captured neuronal representations were significant in delta band (1-4 Hz) for the PMv Cortex as well as other areas (including the electrodes on frontal, temporal and parietal regions). This shows that task-related motor activity (in this case just finger-tapping), in comparison with the rest condition induced an increase in the power density in delta band in PMv Cortex which is responsible for the modulation of human voluntary movements [63]. FC6 (with delta band) seems to be the neuronal region associated with fingers and their movement as it can also be seen in table 4.2 when contrasting M vs R on MSL Day.

4.1.4 EEG Contrasts Illustrated on EEG Map

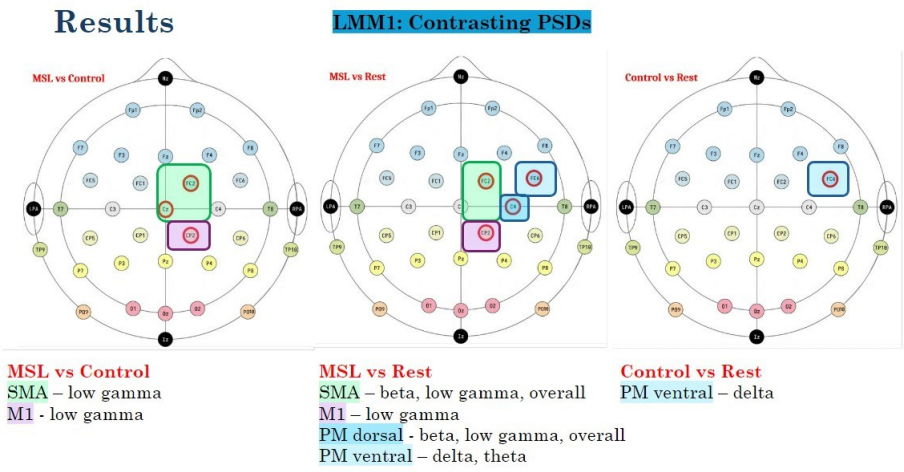

Figure 4.1: Illustration of LMM1 results on EEG 32 channel map

4.2 Group-Level Estimations of Correlation between Longitudinal EEG and MRS

After investigating task-related neuronal representations in PSD using the LMM1, we took advantage of the LMM to investigate if the variations in EEG is modulated by the variations in Glutamate (GLU) during the MSL and Control days. Therefore, LMM2 is used for modeling the PSD longitudinal behaviour as a function of the GLU longitudinal behaviour in SMA and PCC areas for the two days and to test if there is any correlation between the two.

4.2.1 EEG vs MRS Correlation (in SMA) on MSL Day

Table 4.4 shows the results for fitting the PSD values of each electrode and band as a function of the GLU variations in SMA area on MSL day. For an illustration of the results please refer to Figure 4.2.

The EEG electrode FC2 is on the SMA area and is showing a significant correlation with the GLU in SMA area particularly in low gamma band and in overall band. This means the electrical activity associated with the task-related memory traces in SMA has a significant correlation with the underlying metabolite activity i.e. GLU.

Apart from this significant correlation in SMA, we can also see the electrical activity in other regions of the motor network in the left hemisphere, such as CP1 on the M1, FC5 on the PMv Cortex, and CP5 on the Primary Sensory Cortex (S1) showing a significant correlation with the GLU levels in SMA area which might indicate that the mentioned regions might follow the same metabolic activity for the GLU both globally during the whole day as well as under the task condition.

EEG vs MRS Band Specific Oscillations in SMA, Motor and Sensory Regions on MSL Day: In table 4.4, we can see the correlation of EEG (PSD) and MRS (GLU) is in low gamma band as well as the overall band which was also observed in LMM1 when we contrasted M vs R for PSD on MSL day (table 4.2). Previously, glutamate was shown to have a correlation with EEG in gamma band oscillations under a visual task condition in humans [65] We can find a similar correlation in other motor regions such as PMv cortex in low gamma and overall band, and M1 in low gamma band on the left hemisphere (ipsilateral to the training hand). Lastly, in this correlation, we can

ROI	Channel	Band	Correlation	Standard Error	p-value<0.05
SMA	FC2	low gamma	0.582	0.186	0.006
SMA	FC2	all	0.529	0.194	0.014
M1	CP1	low gamma	0.463	0.136	0.018
PMv	FC5	low gamma	0.497	0.216	0.034
PMv	FC5	all	0.5	0.223	0.038
S1	CP5	theta	0.514	0.186	0.013
S1	CP5	alpha	0.482	0.209	0.033
S1	CP5	low gamma	0.577	0.206	0.012
	P3	low gamma	0.372	0.176	0.049

Table 4.4: Results of the Linear Mixed Model (LMM2) for the EEG vs MRS in SMA area on MSL Day

also observe S1 in low gamma band and lower frequency bands (theta and alpha). During finger movements, S1 was shown to be modulated by PM [62] and have interaction with M1 [63].

4.2.2 EEG vs MRS Correlation (in SMA) on Control Day

Table 4.5 shows the results for fitting the PSD values of each electrode and band as a function of the GLU variations in SMA area on Control day. For an illustration of the results please refer to Figure 4.2.

As shown in the table, we cannot see any particular EEG electrode on the SMA area showing correlation with the GLU variations in SMA area as this was the Control day in which participants just performed finger-tapping movements without any sequence learning. However, we can see the electrical activity in other regions of the motor network, i.e. FC6 on the PMv Cortex, showing a significant correlation with the GLU levels in SMA on Control day. As mentioned before, on Control day, we expect to see the PM area as the region which modulates the voluntary motor movement [62, 63], however its correlation with the metabolic activity of the SMA area might indicate that the PM region might follow the same metabolic variations as that of the GLU in SMA area both globally during the whole day as well as under the task condition (finger movements).

EEG vs MRS Band Specific Oscillations in PM on Control Day: In table 4.5, we can see the correlation of EEG (PSD) and MRS (GLU) is in delta band which was also observed in LMM1 when we contrasted C vs R for PSD on Control day (table 4.3). Moreover, the correlation between

ROI	Channel	Band	Correlation	Standard Error	p-value<0.05
PMv	FC6	delta	0.695	0.161	0
PMv	FC6	alpha	0.54	0.189	0.011
Visual	O1	theta	0.613	0.215	0.011
Visual	O1	beta	0.684	0.173	0.001
Visual	O2	alpha	0.461	0.209	0.05
	F3	theta	0.496	0.186	0.042
	Fp1	theta	0.549	0.186	0.033
	P8	theta	0.614	0.182	0.01
	P3	alpha	0.461	0.185	0.023
	T8	theta	0.637	0.207	0.006

Table 4.5: Results of the Linear Mixed Model (LMM2) for the EEG vs MRS in SMA area on Control Day

the PSD and the GLU is also significant in alpha band.

4.2.3 EEG vs MRS Correlation (in PCC) on MSL Day

Table 4.6 shows the results for fitting the PSD values of each electrode and band as a function of the GLU variations in PCC area on MSL day. For an illustration of the results please refer to Figure 4.3.

From the paradigm, we are not expecting to see PCC showing an activation due to the MSL task. and the model didn't capture any correlation for the EEG electrodes on the surface on top of PCC area(such as P3, P4 or Pz).

ROI	Channel	Band	Correlation	Standard Error	p-value<0.05
	P7	low gamma	0.429	0.188	0.033
SMA	Cz	beta	0.43	0.187	0.033

Table 4.6: Results of the Linear Mixed Model (LMM2) for the EEG vs MRS in PCC area on MSL Day

However, it is showing a significant correlation for two other electrodes, P7 which is located around the PCC area on the left hemisphere (which was also observed in table 4.4 for EEG-MRS correlation in SMA on MSL day) and Cz located on the SMA area.

EEG vs MRS Band Specific Oscillations in PCC on Control Day: Both of the electrodes captured in this model are showing to be correlated with glutamate variations in PCC in high frequency

bands, i.e. beta and low gamma, which was mentioned to be task-related on MSL day.

4.2.4 EEG vs MRS Correlation (in PCC) on Control Day

ROI	Channel	Band	Correlation	Standard Error	p-value<0.05
	P4	delta	0.756	0.179	0.009
	P4	beta	0.672	0.173	0.001
	P3	theta	0.528	0.226	0.031
	P3	beta	0.386	0.158	0.029
	T7	delta	0.412	0.174	0.029
	T7	beta	0.51	0.197	0.029
	F7	beta	0.486	0.209	0.032
	F3	theta	0.539	0.217	0.023
PMd	C3	beta	0.477	0.205	0.036
Visual	O2	beta	0.481	0.166	0.012

Table 4.7: Results of the Linear Mixed Model (LMM2) for the EEG vs MRS in PCC area on Control Day

Table 4.7 shows the results for fitting the PSD values of each electrode and band as a function of the GLU variations in PCC area on Control day. For an illustration of the results please refer to Figure 4.3.

From the paradigm, we are not expecting to see PCC showing an activation due to the Control task. However, the model is capturing a significant correlation between the electrical activity of EEG electrodes P3 and P4 located at distance on top of the PCC area with the metabolic activity captured by MRS in PCC during the Control day. We can also see C3 located on PMd Cortex on the left hemisphere having a significant correlation with GLU variations in PCC area. Activation of C3 as the PMd area is expected due to the finger-tapping movements. However, it's correlation with GLU variations in PCC was not expected.

4.2.5 EEG vs MRS Correlations Illustrated on EEG Map

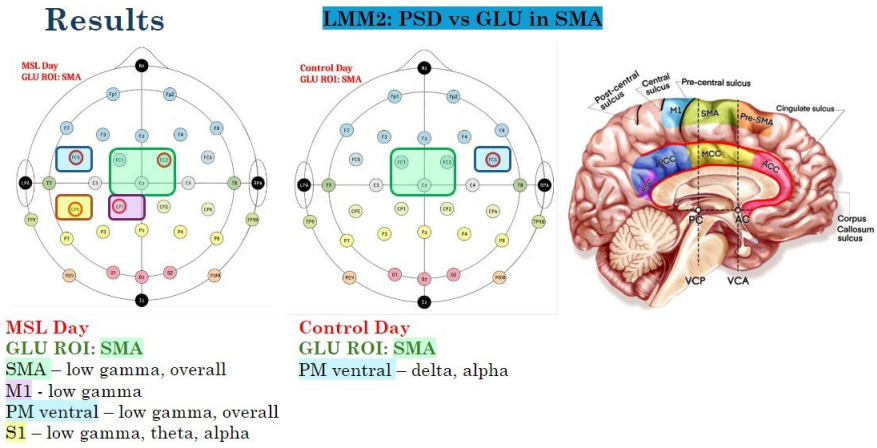

Figure 4.2: Illustration of LMM2 results for SMA on EEG 32 channel map. Figure on the right from [66]

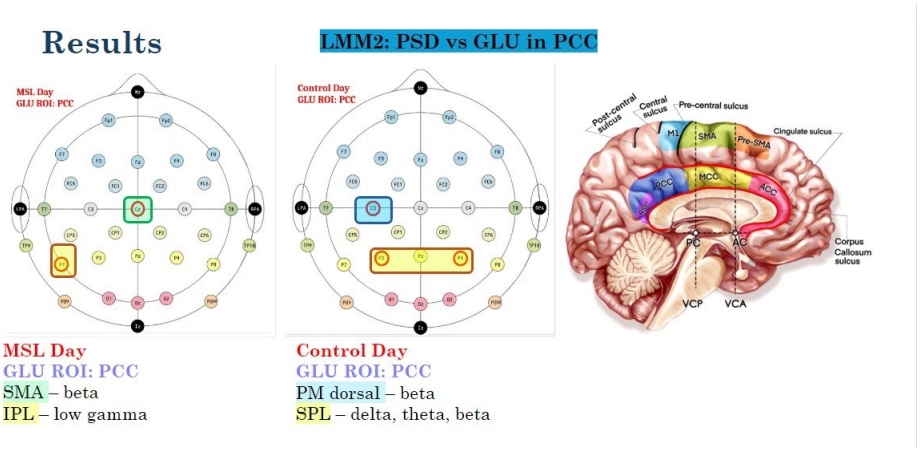

Figure 4.3: Illustration of LMM2 results for PCC on EEG 32 channel map. Figure on the right from [66]

Chapter 5

Discussion and Conclusion

5.1 Discussion

In this study, we investigated human motor skill learning in the form of a motor sequence task to explore the resting state brain modifications induced after the task as well as no learning conditions which included rest, fast stage (or early) modifications and slow stage (or long-term) modifications. We acquired resting state EEG-fMRI and MRS at multiple times during the control and MSL visits from six healthy participants (see the protocol schematic in Figure 2.1). MSL visit included overnight sleep (PSG) acquisition for testing task-related neuronal reactivations in the sleep and potential consolidation process (slow stage).

Findings of a previous study using MRS in motor sequence learning suggested that there is a positive relationship between the glutamate and the motor learning both at rest and during the task (fast stage of learning) [31]. Another study in the same paradigm using fMRI and MRS, also found out that the fast satge glutamate (and GABA) signaling in the Primary Motor area was associated with the long-term (slow stage of learning, after the overnight sleep) structural, functional and behavioral modifications in the brain suggesting the dependence of long-term learning-induced changes or consolidation of the memory on glutamate variations [20]. However, looking at the literature in human studies, we lack evidence supporting the correlations of metabolic and electrical activity of the brain in motor sequence learning (MSL).

In this current thesis, using the data from five subjects, we explored the MSL in terms of the

diurnal changes in electrical activity (acquired from EEG) and glutamate concentrations (acquired from MRS) of the brain in the fast stage during the whole wake period before and after the tasks (diurnal).

Our results for this part of the analysis were two folded: 1- The EEG results contrasting rest, control and MSL conditions, and 2- The longitudinal dynamics of EEG vs MRS.

For the first part, the results of the Linear Mixed Model (LMM) suggested that the EEG power spectrum density (PSD) for MSL vs control shows significant (Table 4.1) low gamma (30-55 Hz) band oscillations in the task-related brain areas particularly in FC2 (on top of the SMA) and CP2 (on top of M1). Considering that the motor sequence learning would require a high cognitive demand and that we removed finger-tapping movements effect, extracting neuronal firings after the task (memory representations or traces) in the task-related regions with low gamma oscillations were expected which is in line with the literature [60, 61].

In the same model, when contrasting MSL vs rest conditions (including the finger-tapping movement effects together with MSL effect), the low gamma band with the same electrodes (FC2 on SMA and CP2 on M1) were still significant (Table 4.2) as well as other bands, such as beta (13-30 Hz) and overall (0.5-55 Hz) bands for both SMA (FC2) and PMd (C4), and delta (1-4 Hz) and theta (4-8 Hz) bands for PMv (FC6) indicating while MSL cognitive demands induce memory traces in low gamma band in SMA and M1, the effect of finger-tapping movement together with MSL can create traces in beta band in SMA and PM (which was also shown in [59]) and in PMv also with delta and theta bands; Here, the PMd (C4, beta, low gamma and overall bands) seems to have traces related to the modulation of the voluntary motor movement [63] and PMv (FC6, delta and theta bands) seems to carry the traces with lower frequency bands related to decision making in finger-tapping movements [64].

Finally, for the first model, with contrasting control vs rest conditions (investigating the effect of finger-tapping movements in the absence of any high cognitive demand for learning) in the same model (Table 4.3), we observed significant memory traces in the PMv area (FC6) in delta band as well as a network of electrodes in other brain regions (such as frontal, parietal and occipital) all in delta band which might indicate the effect of finger-tapping movement without any cognitive demand for sequence learning is in the lowest frequency band.

The above-mentioned EEG related findings in the motor network (including SMA, M1 and PM in all contrasts) were in the contralateral hemisphere to the training hand (left) which is in line with the literature with the same paradigm and different imaging modalities [5, 11, 12, 20, 59].

For the second part of the results, the result of LMM for longitudinal modeling of EEG vs MRS on MSL day in the targeted brain region, SMA, showed a significant correlation (Table 4.4 and Figure 4.2) between the PSD of FC2 (on the SMA) and glutamate levels in SMA in low gamma and overall bands which were also significant in the first model when contrasting MSL vs rest on MSL day for PSD. This indicates that the task-related memory traces induced in SMA in the form of electrical activity are correlated with the underlying glutamate signaling in the same brain region.

Apart from this significant correlation in electrical and metabolic activity in SMA, in the same model, we can also see other electrodes from other motor network regions showing a significant correlation with glutamate dynamics in SMA; These are the regions M1 (CP1, low gamma band), PMv (FC5, low gamma and overall bands) and S1 (CP5, theta, alpha and low gamma). Interestingly, these electrodes are on the left hemisphere ipsilateral to the training hand. From the literature, we know that in stroke studies, impairments in the early phase of MSL were more severe in the contralateral hand than in the ipsilateral hand [67]. In addition, evidence from other studies on the ipsilateral limb to the damaged brain suggests that higher-order planning and organization of learned motor actions is the role of the ipsilateral hemisphere [68].

On Control day, we cannot find any correlation between the electrical and metabolic activity in SMA, however the model is still showing a correlation between electrical activity in PMv (FC6) with the GLU in SMA.

For glutamate dynamics in the PCC area and its correlation with EEG, we did not expect to find any correlation, as the PCC is the area involved in sleep homeostasis; however, the results indicate that glutamate dynamics in PCC has a significant correlation with EEG of the inferior and superior parietal lobs (IPL and SPL) as well as the central electrodes. This correlation is in low gamma and beta bands on MSL day and delta, theta and beta bands on Control day (shown in Tables 4.6 and 4.7 and Figure 4.3).

5.2 Conclusion

In this work, through a motor sequence learning paradigm, we could find the memory traces related to the paradigm in the form of electrical activity read from the scalp electrodes on top of the SMA and M1 areas with gamma band oscillations. Furthermore, we could show that this electrical activity read on top of the SMA has a correlation with diurnal glutamate variations in the SMA in both gamma oscillations and overall band on the MSL day. The other finding of this study is that the diurnal glutamate variations in SMA on the day of MSL have a correlation with the electrical activity read from the electrodes in the ipsilateral motor network (specifically PM, S1, and M1) that could indicate that the underlying motor regions also followed the same glutamate variations.

On day of control, there were no correlations between electrical activity and GLU in SMA; however, electrical activity read on top of contralateral PMv showed to have a correlation with diurnal glutamate variations in SMA in lower frequency bands that could be associated with finger-tapping movements.

That why glutamate variations in SMA are associated with electrical activity in other motor and brain regions is not known. The limitation of MRS is that it only allows data acquisition at one single voxel at a time. However, this might indicate that the other brain regions also follow the same glutamate variations as in SMA. This is the same case for glutamate variations in PCC on both MSL and Control days, for which we did not expect any significant correlation between the glutamate variations and electrical activity; however, the results indicate that there is a correlation. PCC is a deep brain region; Finding a correlation between the electrical activity of the centroparietal lobe and the variations of glutamate in PCC could indicate that in the cortex beneath those electrodes, glutamate levels follow the same trend as in PCC.

For implementing the protocol, we suggested a fast way of measuring the EEG 10-20 system by aligning an EEG cap with the reference points (the nasion, the inion and the two preaurical points) and marking the place of electrodes.

Bibliography

[1] D. B. Willingham, "A neuropsychological theory of motor skill learning." Psychological Review, vol. 105, pp. 558–584, 1998.

[2] M. P. Walker, "A refined model of sleep and the time course of memory formation," Behavioral and Brain Sciences, vol. 28, pp. 51–64, 02 2005.

[3] A. Karni, G. Meyer, C. Rey-Hipolito, P. Jezzard, M. M. Adams, R. Turner, and L. G. Ungerleider, "The acquisition of skilled motor performance: Fast and slow experience-driven changes in primary motor cortex," Proceedings of the National Academy of Sciences, vol. 95, pp. 861–868, 02 1998.

[4] E. Tulving, "How many memory systems are there?" American Psychologist, vol. 40, pp. 385–398, 1985.

[5] J. Doyon, E. Gabitov, S. Vahdat, O. Lungu, and A. Boutin, "Current issues related to motor sequence learning in humans," Current Opinion in Behavioral Sciences, vol. 20, pp. 89–97, 04 2018.

[6] M. Korman, J. Doyon, J. Doljansky, J. Carrier, Y. Dagan, and A. Karni, "Daytime sleep condenses the time course of motor memory consolidation," Nature Neuroscience, vol. 10, pp. 1206–1213, 08 2007.

[7] W. Muellbacher, U. Ziemann, J. Wissel, N. Dang, M. Kofler, S. Facchini, B. Boroojerdi, W. Poewe, and M. Hallett, "Early consolidation in human primary motor cortex," Nature, vol. 415, pp. 640–644, 01 2002.

[8] T. Brashers-Krug, R. Shadmehr, and E. Bizzi, “Consolidation in human motor memory,” Nature, vol. 382, pp. 252–255, 07 1996.

[9] M. P. Walker, T. Brakefield, J. Allan Hobson, and R. Stickgold, “Dissociable stages of human memory consolidation and reconsolidation,” Nature, vol. 425, p. 616–620, 10 2003.

[10] A. Karni, G. Meyer, P. Jezzard, M. M. Adams, R. Turner, and L. G. Ungerleider, “Functional mri evidence for adult motor cortex plasticity during motor skill learning,” Nature, vol. 377, pp. 155–8, 1995.

[11] J. Doyon and H. Benali, “Reorganization and plasticity in the adult brain during learning of motor skills,” Current Opinion in Neurobiology, vol. 15, pp. 161–167, 04 2005.

[12] B. Pinsard, A. Boutin, E. Gabitov, O. Lungu, H. Benali, and J. Doyon, “Consolidation alters motor sequence-specific distributed representations,” eLife, 03 2019.

[13] T. Andrillon, Y. Nir, R. J. Staba, F. Ferrarelli, C. Cirelli, G. Tononi, and I. Fried, “Sleep spindles in humans: Insights from intracranial eeg and unit recordings,” Journal of Neuroscience, vol. 31, pp. 17 821–17 834, 12 2011.

[14] M. P. Walker, T. Brakefield, A. Morgan, J. Hobson, and R. Stickgold, “Practice with sleep makes perfect,” Neuron, vol. 35, pp. 205–211, 07 2002.

[15] S. FOGEL, C. SMITH, and K. COTE, “Dissociable learning-dependent changes in rem and non-rem sleep in declarative and procedural memory systems,” Behavioural Brain Research, vol. 180, pp. 48–61, 06 2007.

[16] A. Boutin, B. Pinsard, A. Boré, J. Carrier, S. M. Fogel, and J. Doyon, “Transient synchronization of hippocampo-striato-thalamo-cortical networks during sleep spindle oscillations induces motor memory consolidation,” NeuroImage, vol. 169, pp. 419–430, 04 2018.

[17] T. R. Soderling and V. A. Derkach, “Postsynaptic protein phosphorylation and ltp,” Trends in Neurosciences, vol. 23, pp. 75–80, 02 2000.

[18] G. Tononi and C. Cirelli, “Sleep function and synaptic homeostasis,” Sleep Medicine Reviews, vol. 10, pp. 49–62, 02 2006.

[19] ——, “Sleep and the price of plasticity: From synaptic and cellular homeostasis to memory consolidation and integration,” Neuron, vol. 81, pp. 12–34, 01 2014.

[20] T. Eisenstein, E. Furman-Haran, and A. Tal, “Early excitatory-inhibitory cortical modifications following skill learning are associated with motor memory consolidation and plasticity overnight,” Nature Communications, vol. 15, 01 2024.

[21] M. Rodriguez, M. Sabate, C. Rodriguez-Sabate, and I. Morales, “The role of non-synaptic extracellular glutamate,” Brain Research Bulletin, vol. 93, pp. 17–26, 2013.

[22] B. Pál, “Involvement of extrasynaptic glutamate in physiological and pathophysiological changes of neuronal excitability,” Cellular and Molecular Life Sciences, vol. 75, pp. 2917–2949, 05 2018.

[23] H. Kida and D. Mitsushima, “Mechanisms of motor learning mediated by synaptic plasticity in rat primary motor cortex,” Neuroscience Research, vol. 128, pp. 14–18, 03 2018.

[24] E. A. Woodcock, C. Anand, D. Khatib, V. A. Diwadkar, and J. A. Stanley, “Working memory modulates glutamate levels in the dorsolateral prefrontal cortex during 1h fmrs,” Frontiers in Psychiatry, vol. 9, 03 2018.

[25] M. B. Dash, C. L. Douglas, V. V. Vyazovskiy, C. Cirelli, and G. Tononi, “Long-term homeostasis of extracellular glutamate in the rat cerebral cortex across sleep and waking states,” Journal of Neuroscience, vol. 29, p. 620–629, 01 2009.

[26] S. Mangia, I. Tkáč, R. Gruetter, V. , B. Maraviglia, and K. Ugurbil, “Sustained neuronal activation raises oxidative metabolism to a new steady-state level: Evidence from ¡sup¿1¡/sup¿h nmr spectroscopy in the human visual cortex,” Journal of Cerebral Blood Flow Metabolism, vol. 27, pp. 1055–1063, 05 2007.

[27] B. Schaller, L. Xin, K. O’Brien, A. W. Magill, and R. Gruetter, “Are glutamate and lactate increases ubiquitous to physiological activation? a 1h functional mr spectroscopy study during motor activation in human brain at 7tesla,” NeuroImage, vol. 93, pp. 138–145, 06 2014.

[28] C. Sampaio-Baptista, N. Filippini, C. J. Stagg, J. Near, J. Scholz, and H. Johansen-Berg, "Changes in functional connectivity and gaba levels with long-term motor learning," NeuroImage, vol. 106, pp. 15–20, 02 2015.

[29] J. Kolasinski, E. L. Hinson, A. P. Divanbeighi Zand, A. Rizov, U. E. Emir, and C. J. Stagg, "The dynamics of cortical gaba in human motor learning," The Journal of Physiology, vol. 597, pp. 271–282, 11 2018.

[30] K. Kurcyus, E. Annac, N. M. Hanning, A. D. Harris, G. Oeltzschner, R. Edden, and V. Riedl, "Opposite dynamics of gaba and glutamate levels in the occipital cortex during visual processing," The Journal of Neuroscience, vol. 38, pp. 9967–9976, 10 2018.

[31] T. K. Bell, A. R. Craven, K. Hugdahl, R. Noeske, and A. D. Harris, "Functional changes in gaba and glutamate during motor learning," eneuro, vol. 10, pp. ENEURO.0356–20.2023, 02 2023.

[32] C. Volk, V. Jaramillo, R. R. Merki, R. L. O'Gorman, and R. Huber, "Diurnal changes in glutamate + glutamine levels of healthy young adults assessed by proton magnetic resonance spectroscopy," vol. 39, pp. 3984–3992, 10 2018.

[33] S. M. Fogel, G. Albouy, C. Vien, R. Popovicci, B. R. King, R. Hoge, S. Jbabdi, H. Benali, A. Karni, P. Maquet, J. Carrier, and J. Doyon, "fmri and sleep correlates of the age-related impairment in motor memory consolidation," Human Brain Mapping, vol. 35, pp. 3625–3645, 12 2013.

[34] G. Cona and C. Semenza, "Supplementary motor area as key structure for domain-general sequence processing: A unified account," Neuroscience Biobehavioral Reviews, vol. 72, pp. 28–42, 01 2017.

[35] D. Klitsinikos, J. O. Ekert, A. Carels, and G. Samandouras, "Mapping and anatomo-surgical techniques for sma-cingulum-corpus callosum gliomas; how i do it," Acta Neurochir, 03 2021.

[36] B. L. Foster, S. R. Koslov, L. Aponik-Gremillion, M. E. Monko, B. Y. Hayden, and S. R. Heilbronner, "A tripartite view of the posterior cingulate cortex," Nature Reviews Neuroscience, vol. 24, p. 173–189, 03 2023.

[37] R. Leech and D. J. Sharp, "The role of the posterior cingulate cortex in cognition and disease," Brain, vol. 137, pp. 12–32, 07 2013.

[38] R. Leech and J. Smallwood, "The posterior cingulate cortex: Insights from structure and function," Handbook of Clinical Neurology, vol. 166, p. 73–85, 2019.

[39] M. van der Graaf, "In vivo magnetic resonance spectroscopy: basic methodology and clinical applications," European Biophysics Journal, vol. 39, pp. 527–540, 08 2009.

[40] H. Zhu and P. B. Barker, "Mr spectroscopy and spectroscopic imaging of the brain," Methods in Molecular Biology, vol. 711, pp. 203–226, 12 2010.

[41] T. Bollinger and U. Schibler, "Circadian rhythms – from genes to physiology and disease," Swiss Medical Weekly, 07 2014.

[42] A. Delorme and S. Makeig, "Eeglab: an open source toolbox for analysis of single-trial eeg dynamics including independent component analysis," Journal of Neuroscience Methods, vol. 134, no. 1, pp. 9–21, 2004.

[43] D. Bates, M. Mächler, B. Bolker, and S. Walker, "Fitting linear mixed-effects models using lme4," Journal of Statistical Software, vol. 67, 2015.

[44] M. K. Egan, R. Larsen, J. Wirsich, B. P. Sutton, and S. Sadaghiani, "Safety and data quality of eeg recorded simultaneously with multi-band fmri," PLOS ONE, vol. 16, p. e0238485, 07 2021.

[45] J. Malmivuo and R. Plonsey, Bioelectromagnetism : Principles and Applications of Bioelectric and Biomagnetic Fields. New York Oxford University Press -10-05, 1995.

[46] J. Kuratani, P. L. Pearl, L. R. Sullivan, R. M. S. Riel-Romero, J. Cheek, M. M. Stecker, D. S. J. Orta, O. Selioutski, S. R. Sinha, F. W. Drislane, and T. N. Tsuchida, "American clinical neurophysiology society guideline 5: Minimum technical standards for pediatric electroencephalography," The Neurodiagnostic Journal, vol. 56, pp. 266–275, 10 2016.

[47] D. Brigham, Y. Shah, K. Singh, I. Pavkovic, S. Karkare, and S. V. Kothare, "Comparison of artifacts between paste and collodion method of electrode application in pediatric eeg," Clinical Neurophysiology Practice, vol. 5, pp. 12–15, 2020.

[48] G. Lin, J. Zhang, Y. Liu, T. Gao, W. Kong, X. Lei, and T. Qiu, "Ballistocardiogram artifact removal in simultaneous eeg-fmri using generative adversarial network," Journal of Neuroscience Methods, vol. 371, p. 109498, 04 2022.

[49] K. J. Mullinger, P. Castellone, and R. Bowtell, "Best current practice for obtaining high quality eeg data during simultaneous fmri," Journal of Visualized Experiments, 06 2013.

[50] M. Bullock, G. D. Jackson, and D. F. Abbott, "Artifact reduction in simultaneous eeg-fmri: A systematic review of methods and contemporary usage," Frontiers in Neurology, vol. 12, 2021.

[51] W. X. Yan, K. J. Mullinger, M. J. Brookes, and R. Bowtell, "Understanding gradient artefacts in simultaneous eeg/fmri," NeuroImage, vol. 46, no. 2, pp. 459–471, 2009.

[52] J. Jorge, F. Grouiller, Özlem Ipek, R. Stoermer, C. M. Michel, P. Figueiredo, W. van der Zwaag, and R. Gruetter, "Simultaneous eeg–fmri at ultra-high field: Artifact prevention and safety assessment," NeuroImage, vol. 105, pp. 132–144, 2015.

[53] P. J. Allen, O. Josephs, and R. Turner, "A method for removing imaging artifact from continuous eeg recorded during functional mri," NeuroImage, vol. 12, no. 2, pp. 230–239, 2000.

[54] S. Makeig, A. Bell, T.-P. Jung, and T. J. Sejnowski, "Independent component analysis of electroencephalographic data," Advances in neural information processing systems, vol. 8, 1995.

[55] T.-P. Jung, S. Makeig, C. Humphries, T.-W. Lee, M. J. Mckeown, V. Iragui, and T. J. Sejnowski, "Removing electroencephalographic artifacts by blind source separation," Psychophysiology, vol. 37, no. 2, pp. 163–178, 2000.

[56] C. Mulert and L. Lemieux, EEG-fMRI Physiological Basis, Technique, and Applications. Springer Berlin Heidelberg, 2010.

[57] L. J. Gabard-Durnam, C. Wilkinson, K. Kapur, H. Tager-Flusberg, A. R. Levin, and C. A. Nelson, "Longitudinal eeg power in the first postnatal year differentiates autism outcomes," Nature Communications, vol. 10, 09 2019.

[58] K. Ezzatdoost, "Relating the circadian dynamics of cortical glutamate to human motor plasticity: a trimodal mrs-eeg-fmri imaging study," Concordia.ca, 06 2024.

[59] S. Dyck and C. Klaes, "Training-related changes in neural beta oscillations associated with implicit and explicit motor sequence learning," Scientific Reports, vol. 14, 03 2024.

[60] M. Nowak, C. Zich, and C. J. Stagg, "Motor cortical gamma oscillations: What have we learnt and where are we headed?" Current Behavioral Neuroscience Reports, vol. 5, pp. 136–142, 04 2018.

[61] D. Cheyne and P. Ferrari, "Meg studies of motor cortex gamma oscillations: evidence for a gamma "fingerprint" in the brain?" Frontiers in Human Neuroscience, vol. 7, 2013.

[62] M. S. Christensen, J. Lundbye-Jensen, S. S. Geertsen, T. H. Petersen, O. B. Paulson, and J. B. Nielsen, "Premotor cortex modulates somatosensory cortex during voluntary movements without proprioceptive feedback," Nature Neuroscience, vol. 10, pp. 417–419, 03 2007.

[63] H. Sun, T. Blakely, F. Darvas, J. D. Wander, L. C. Johnson, D. K. Su, K. J. Miller, E. E. Fetz, and J. G. Ojemann, "Sequential activation of premotor, primary somatosensory and primary motor areas in humans during cued finger movements," Clinical Neurophysiology, vol. 126, pp. 2150–2161, 11 2015.

[64] J. Körmendi, E. Ferentzi, B. Weiss, and Z. Nagy, "Topography of movement-related delta and theta brain oscillations," Brain Topography, vol. 34, pp. 608–617, 06 2021.

[65] N. Lally, P. G. Mullins, M. V. Roberts, D. Price, T. Gruber, and C. Haenschel, "Glutamatergic correlates of gamma-band oscillatory activity during cognition: A concurrent er-mrs and eeg study," NeuroImage, vol. 85, pp. 823–833, 01 2014.

[66] F. Gong, J. Liu, Q. Song, Y. Zhong, H. Chen, and J. Wu, "Surgical techniques and function outcome for cingulate gyrus glioma, how we do it," Frontiers in Oncology, vol. 12, 09 2022.

[67] M. G. Beldarrain, J. Grafman, A. Pascual-Leone, and J. C. Garcia-Monco, "Procedural learning is impaired in patients with prefrontal lesions," Neurology, vol. 52, pp. 1853–1853, 06 1999.

[68] L. A. Boyd and C. J. Winstein, "Implicit motor-sequence learning in humans following unilateral stroke: the impact of practice and explicit knowledge," Neuroscience Letters, vol. 298, pp. 65–69, 01 2001.